Geomorphology 505 (2026) 110319

Contents lists available at ScienceDirect

Geomorphology

journal homepage: www.journals.elsevier.com/geomorphology

Morphometry and characteristics of subglacial meltwater corridors within the Finnish Lake District Ice Lobe of the former Fennoscandian Ice Sheet – Implications for subglacial hydrology and ice lobe dynamics

Juulia J. Kautto [a,*], Joni K. Mäkinen [a], Antti E.K. Ojala [a,b]

[a] Department of Geography and Geology, University of Turku, FI-20014 Turun yliopisto, Finland
[b] Geological Survey of Finland, P.O. Box 96, (Vuorimiehentie 5), FI-02151 Espoo, Finland

ARTICLE INFO

Keywords:
Subglacial hydrology
Fennoscandian Ice Sheet
Glacial geomorphology
Subglacial meltwater corridors
Subglacial lakes
Eskers

ABSTRACT

Detailed knowledge of subglacial hydrology is essential for understanding past and future ice sheet behavior, yet direct observations in contemporary settings remain challenging. Subglacial meltwater corridors (SMCs) are composite landforms that record various forms of subglacial drainage and, together with eskers, provide key constraints for past ice sheet reconstructions and future drainage modeling. In the present study, we investigated SMCs in the Finnish Lake District Ice Lobe (FLDIL) of the former Fennoscandian Ice Sheet (FIS). By examining their morphometry, relief types, and association with eskers, our aim was to evaluate how their characteristics relate to regional variations in topography, landform distribution and ice sheet dynamics. Our results demonstrate that bedrock topography, the thickness of glacial overburden, and the presence of potential subglacial lakes exert major control on SMC form and distribution. The spatial pattern of SMC–esker associations also reveals distinct regional variations in dominant drainage modes. These findings support earlier hypotheses of ice flow reorganization events driven by changes in ice sheet configuration and proglacial water depth during deglaciation. In addition, our results highlight significant differences between the dynamics of the western and eastern sectors of the FLDIL lobe and provide new insights into paleo-subglacial lakes as active components of the subglacial drainage system in the Finnish sector of the FIS.

1. Introduction

Dynamic variations in basal meltwater routing, storage and drainage exert control on the flow of mountain glaciers and ice sheets (Livingstone et al., 2022). In temperate environments, where the majority of meltwater generation is surface-driven, the meltwater supply to the subglacial domain can vary seasonally (Bartholomew et al., 2010), diurnally (Shepherd et al., 2009), or due to sudden outbursts from supra- or subglacial water storages (Das et al., 2008; Palmer et al., 2015). Meltwater generated at the ice surface frequently ponds in supraglacial lakes which can drain rapidly and deliver large quantities of meltwater to the bed via crevasses and moulins (Das et al., 2008; Dow et al., 2015). Stable and active subglacial lakes can act as longer-term storages or modulate subglacial drainage through their fill-and-drain cycles (Willis et al., 2015; Livingstone et al., 2022). The volume of meltwater and the configuration of the prevailing drainage system at the ice-bed interface directly affects variations in effective pressure (ice pressure – water pressure), which in turn governs patterns in ice velocity and ultimately contributes to ice sheet mass loss and sea-level rise (Schoof, 2010; Greenwood et al., 2016; Davison et al., 2019).

Meltwater flow at the ice-bed interface has traditionally been categorized into two end-member configurations. Distributed (or "slow" / "inefficient") drainage refers to configurations of water flow over a larger portion of the bed, such as thin films, linked cavities, shallow canals or porous flow within sediments (Fountain and Walder, 1998). Channelized (or "fast" / "efficient") system, on the other hand, refers to drainage concentrated into discrete channels or conduits cut either into the overlying ice or the substrate material (Hooke, 2019). Studies from alpine glaciers (e.g. Hubbard and Nienow, 1997) have shown that distributed drainage systems are typically associated with higher water pressures and enhanced ice motion, whereas in a channelized system the subglacial water pressure is reduced, leading to reduced ice flow velocity. While the existence of transitional modes between these end-member configurations has been made evident (Andrews et al., 2014;

* Corresponding author.
E-mail address: jujokau@utu.fi (J.J. Kautto).

https://doi.org/10.1016/j.geomorph.2026.110319
Received 19 December 2025; Received in revised form 5 April 2026; Accepted 6 April 2026
Available online 8 April 2026

Hoffman et al., 2016; Davison et al., 2019), the ways in which these different modes of drainage interact with each other and evolve in space and time are complex and remain poorly understood in contemporary glacial environments (Simkins et al., 2022).

Studies of paleo-ice sheet beds and landforms allow the reconstruction of past ice sheet dynamics, offering glimpses of the drainage systems which operated beneath them (Greenwood et al., 2016). Eskers, erosional channels and tunnel valleys have long been identified as remnant traces of channelized drainage preserved in the landform record and have been used to reconstruct past ice sheet behavior (e.g. Punkari, 1980; Greenwood et al., 2007; Storrar et al., 2014). Additionally, on the bed of the former Laurentide Ice Sheet, elongated zones containing both erosional and depositional landforms have been connected to subglacial meltwater drainage. These zones have been variably referred to as meltwater corridors, glaciofluvial corridors and erosional corridors (e.g. St-Onge, 1984; Rampton, 2000; Utting et al., 2009; Burke et al., 2012).

The availability of high-resolution LiDAR-based digital elevation models (DEMs) has revealed the widespread presence of such zones across the beds of the former Fennoscandian (FIS) and Laurentide Ice Sheets (Peterson et al., 2017; Peterson and Johnson, 2018; Lewington et al., 2019, 2020; Ahokangas et al., 2021; Dewald et al., 2022). These subglacial meltwater corridors (SMCs) (Fig. 1) are composite records of varying subglacial meltwater drainage configurations, ranging from channelized landforms to distinct tracts of hummocks, murtoos and murtoo-related landforms (Ojala et al., 2021; Dewald et al., 2022). SMCs can be up to 100s of km long and 100s to 1000s of m wide (Vérité et al., 2024a). They vary in relief, displaying both negative and positive morphologies (Peterson and Johnson, 2018), and are typically found incised in till (Vérité et al., 2024a). SMCs have also been frequently observed to contain or connect to eskers (Dewald et al., 2022). Moreover, they have been linked to potential subglacial lake locations (Burke et al., 2012; Ahokangas et al., 2021) and water blister imprints formed by rapid supraglacial water outbursts (Mäkinen et al., 2023b). Consequently, SMCs have been interpreted to record varying forms of interconnected drainage systems (Lewington et al., 2020; Vérité et al., 2024a). These include transitional modes which fall between the classic end-member configurations, often termed as "semi-distributed" systems (Mäkinen et al., 2017; Hovikoski et al., 2023). Although the significance of subglacial meltwater drainage studies via paleo-ice sheet beds is well established, further information on the spatiotemporal variations and interactions between different drainage system components is needed to apply this knowledge when assessing the basal characteristics hidden beneath contemporary ice sheets.

The purpose of this study is to investigate the properties and genesis of SMCs within the Finnish Lake District Ice Lobe (FLDIL) in Central Finland. The region constituted a significant part of the former FIS and provides an interesting setting for multiple reasons. The FLDIL has a distinct structure consisting of an ice stream trunk and a lobate part expressed in a well-preserved landform record. The FLDIL retreated rapidly following the Younger Dryas stadial (c. 11.6–11.7 cal. Kyr BP) (Stroeven et al., 2016; Lunkka et al., 2021). The abundance of eskers, subglacial meltwater routes (SMRs) and murtoos (Ahokangas et al., 2021; Ojala et al., 2021), combined with the substantial sediment volume of the I–II Salpausselkä ice-marginal complexes marking its Younger Dryas extent (Palmu et al., 2026), attests to significant meltwater drainage during deglaciation under conditions which may have resembled those observed in southwestern Greenland today (Greenwood et al., 2016).

By using high-resolution LiDAR-based DEMs as the primary tool, we aim to: (i) describe the morphometric variability and spatial distribution of SMCs within the FLDIL and present their linkage to regional geomorphology, (ii) study the interplay between SMCs and the esker system, and (iii) discuss the results in the context of regional ice sheet dynamics during the Late Weichselian to Early Holocene deglaciation.

2. Study area

During the latest phases of the last deglaciation (c. 13–10 cal. Kyr BP), the Finnish sector of the FIS was divided into several ice lobe provinces and interlobate regions (Fig. 2) (Punkari, 1980; Palmu et al., 2021). The FLDIL was located in Central Finland and covered ~65,000 km^2. It consisted of a well-defined ice stream trunk and a lobate part, which was likely divided into two sub-lobes separated by the Suonenjoki–Punkaharju esker (Palmu et al., 2021). The I and II Salpausselkä ice-marginal complexes were deposited during the Younger Dryas (12.9–11.7 cal. Kyr BP) (cf. Stroeven et al., 2016), during which several stand-still, retreat and readvance phases existed, although the exact extent and timing of them is not unequivocally constrained. Suggestions for the extent of the initial retreat from the I Salpausselkä have varied between 30 and 80 km (Lunkka et al., 2021). Deposition of the II Salpausselkä and the onset of the Holocene Epoch at 11.65 cal. Kyr BP (11.7 kyr b2k) (Walker et al., 2009) was followed relatively rapid and continuous margin retreat, during which the FLDIL lobe terminated partly on land and partly in shallow water (<50 m deep) (Ojala et al., 2013). No evidence of major standstills or readvances have been mapped in the lobate part, and landforms indicating ice margin positions are sporadic up until the town of Pieksämäki and the Lake Keitele area (Dulfer et al., 2026). Evidence of minor readvance events have mainly been documented along the eastern margin of the FLDIL trunk, such as those at Pielavesi (Glückert, 1974) and the Pihtipudas–Pyhäjärvi area (Mäkelä, 1988), and the lack of marginal formations on the western side has been inferred to denote differences in the dynamic behavior of the western and eastern flow corridors (Mäkelä, 1988). The rate of retreat decreased around the Suomenselkä watershed region (Fig. 2C), and Ahokangas and Mäkinen (2014) suggested that the ice flow reorganized into three distinct ice-flow zones at this time. The ice continued to retreat rapidly northwest of the Suomenselkä toward the Bothnian Bay in progressively deeper water (50–200 m deep) (Ojala et al., 2013). The study area was ice free at approximately 10.1–10.2 cal. Kyr BP (Stroeven et al., 2016).

The FLDIL lies predominantly on Precambrian crystalline bedrock overlain by a relatively thin sediment cover consisting of till (c. 1–10 m), glacifluvial sediments and postglacial deposits (Fig. 2A). Aside from the lower lying terrain with large lake basins proximal to the II Salpausselkä, the region on the eastern side of the FLDIL lobe is mostly dominated by rugged topography. The western side is characterized by the extensive Pieksämäki drumlin field (see Glückert, 1973) distal to the Toivakka–Konnevesi bedrock region. Based on Ahokangas et al. (2021) SMRs in the FLDIL lobe largely mirror the orientation of eskers, with some major deviations only in the vicinity of the Jaamankangas interlobate complex. Murtoos and murtoo-related landforms (see Table 1) in the region are especially frequent within the eastern sub-lobe (Ojala et al., 2021) and distal to bedrock regions 40 to 60 km up-ice from the II Salpausselkä (cf. Hepburn et al., 2024), while SMRs composed of hummocky topography typically occur closer to the lobe margin (Ahokangas et al., 2021). Landscape within the Keitele drumlin field southeast of the Suomenselkä (see Glückert, 1973) varies between drumlinized uplands and lake-covered terrain with notably fewer mapped murtoos and SMRs overall (Ahokangas et al., 2021; Ojala et al., 2021). Northwest of the Suomenselkä the terrain is markedly different with southeast oriented, longitudinal bands of hummocky and ribbed moraine fields and adjacent streamlined till plains (incl. MSGLs indicative of ice streaming; see Clark, 1993). Majority of SMRs, murtoos and murtoo-related landforms in the region are located within the ribbed and hummocky terrain and appear in connection to the major esker chains situated between the ice-flow zones (Ahokangas and Mäkinen, 2014; Ahokangas et al., 2021).

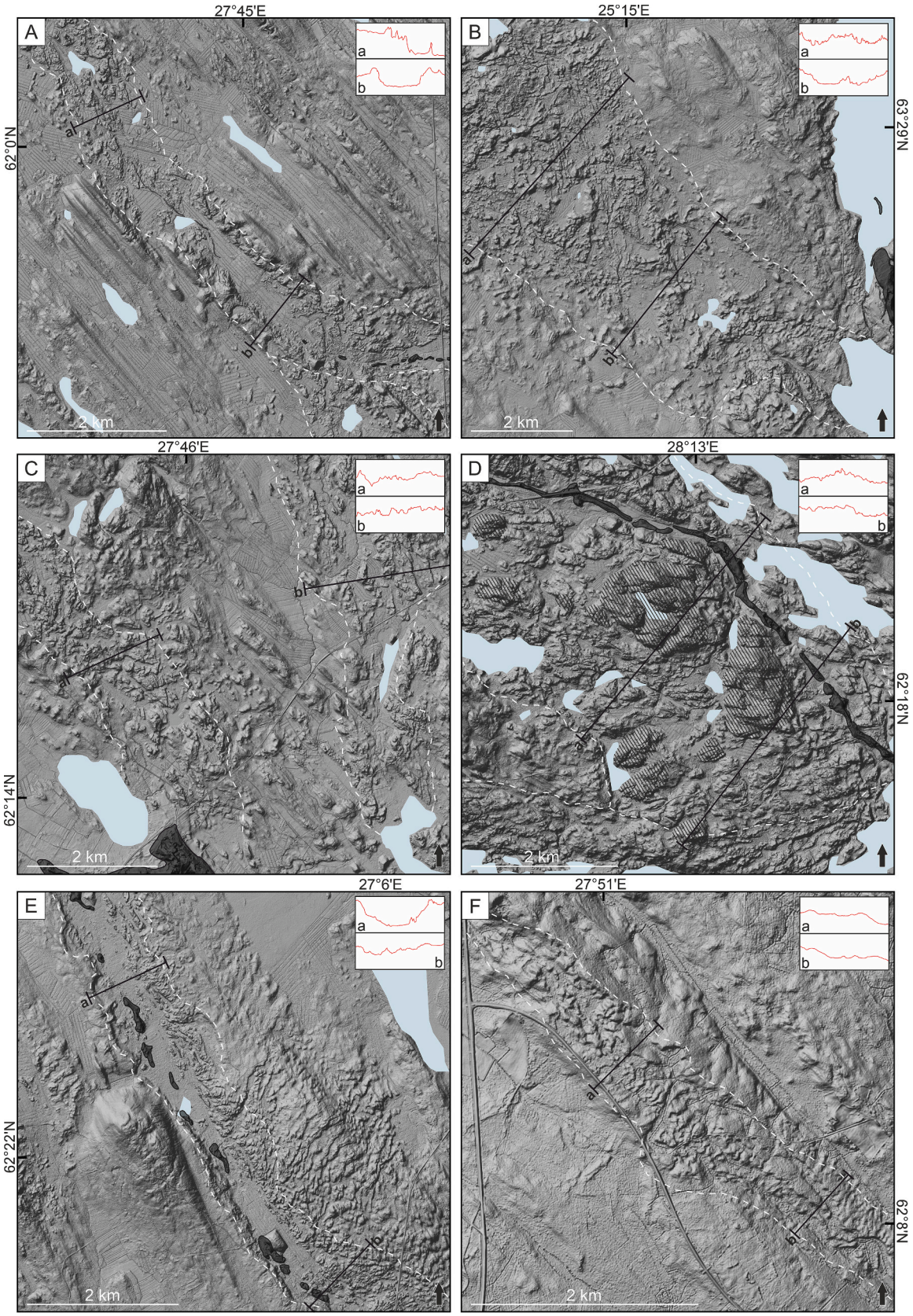

(caption on next page)

Fig. 1. Examples of different types of subglacial meltwater corridors (SMCs) identifiable within the Finnish lake District Ice Lobe (FLDIL) from a LiDAR-based DEM (© National Land Survey of Finland). Ice flow was roughly toward southeast in each example. Eskers are depicted as dark gray polygons (Geological Survey of Finland, 2021). SMC margins and cross-sections have been slightly simplified for visualization purposes. A) A positive-relief SMC with murtoos transitioning into a negative-relief corridor (see Peterson and Johnson, 2018) with an inset esker. B) A negative-relief SMC with smoothed margins containing murtoos, hummocks and erosional escarpments (Ojala et al., 2021) within a heavily modified ribbed moraine field (see Vérité et al., 2022). The area represents a meltwater complex that likely consists of at least two adjacent corridors which appear to merge and connect to an esker down-ice. C) Two positive-relief SMCs with murtoos and escarpments connecting to an esker. D) SMC section with bedrock-controlled relief containing murtoos, small hummocks and bedrock outcrop areas. An esker cross-cuts through the corridor. Prominent bedrock areas are indicated with hashed line pattern. E) A negative-relief SMC with an inset esker and crenulated margins visible at cross-section a (cf. Dewald et al., 2022). F) A short and narrow SMC with indistinct relief and smooth appearance containing hummocks and small channels. The SMC has no apparent connection to an esker.

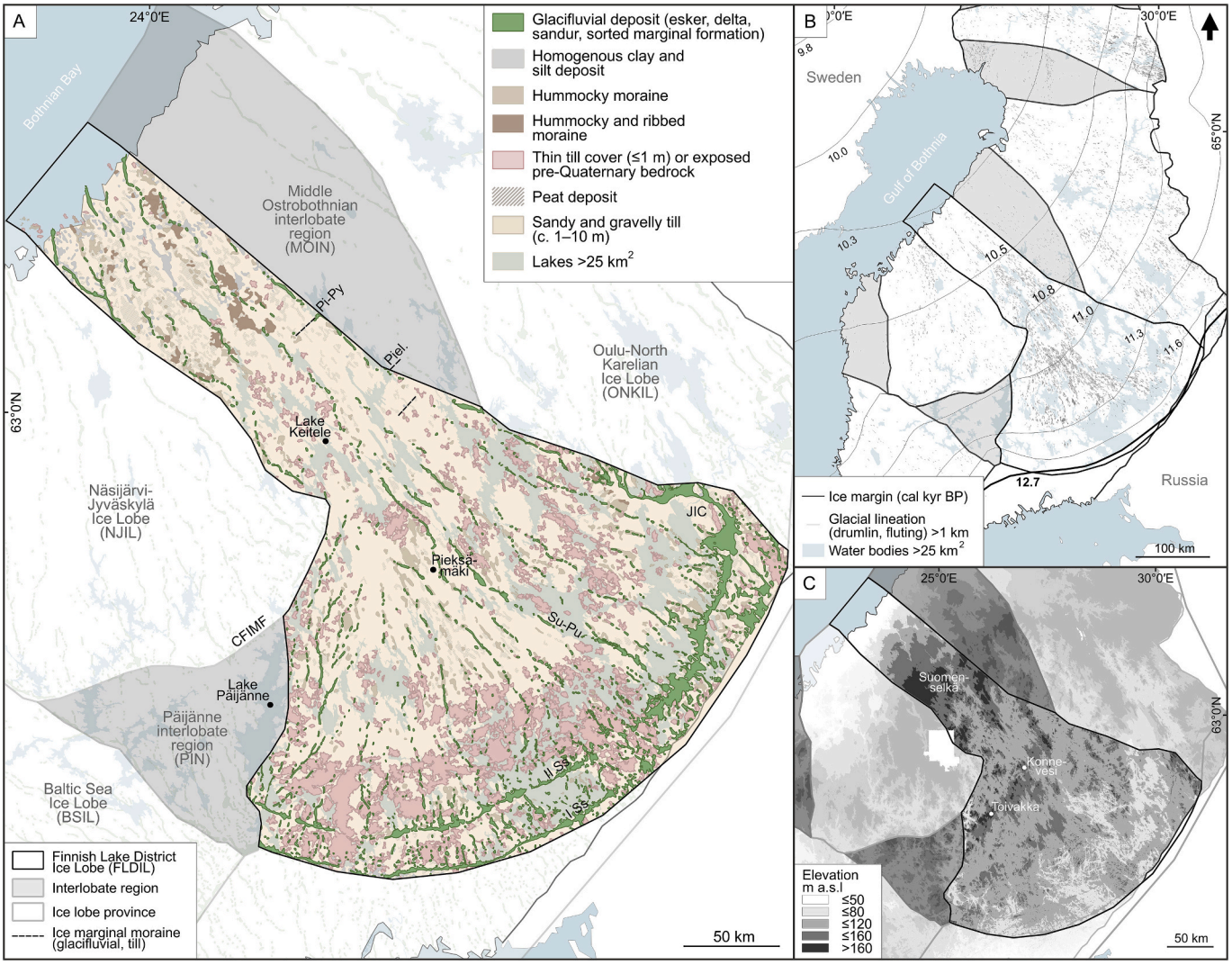

Fig. 2. A) Study area map depicting the Superficial deposits of Finland 1:1000000 (Geological Survey of Finland, 2016, modified). Notice that the hummocky moraine class also contains landform tracts of hummocks and murtoos which have subsequently been associated with SMCs. The Glaciodynamic areas of Finland are based on Palmu et al. (2021). Abbreviations used: I–II Ss (I–II Salpausselkä), JIC (Jaamankangas interlobate complex), CFIMF (Central Finland Ice Marginal Formation), Su–Pu (Suonenjoki–Punkaharju esker), Piel. (Pielavesi end moraine) (Glückert, 1974) and Pi–Py (Pihtipudas–Pyhäjärvi end moraine) (Mäkelä, 1988). B) Location of the study area in Central Finland. Selected ice sheet retreat isochrons (cal kyr BP., Stroeven et al., 2016) and glacial lineations (>1 km in length) (Geological Survey of Finland, 2021) are depicted. C) LiDAR-based DEM of the Finnish Lake District Ice Lobe (© National Land Survey of Finland).

3. Materials and methods

3.1. Data sources and mapping approach

The mapping was based on a high-resolution airborne LiDAR-based DEM (2 m grid / ~0.3 vertical accuracy) and a hillshade with multidirectional oblique weighting (MDOW) (Jennes, 2013) and slope derivatives (Palmu et al., 2015; Putkinen et al., 2017). The previous mapping of SMRs in Finland by Ahokangas et al. (2021) provided an essential starting point for the present study. The term "SMR" has been used to refer to all traces of subglacial meltwater activity, including eskers and subglacial channels of varying scales. In the present study, we will use the term "subglacial meltwater corridor" (SMC) following the hierarchical classification of Dewald et al. (2022), which encompasses all identifiable subglacial landform tracts and potential tunnel valleys, but excludes esker ridges and subglacial channels. The murtoo routes

Table 1
Summary of the criteria used when delineating SMCs. The criteria are based on the observations of typical SMC landforms and characteristics (e.g. Vérité et al., 2024a).

Criteria	Description
Texture	Difference between the usually smoother, surrounding till surface and the rough texture within SMCs (e.g. Vérité et al., 2024a).
Erosional margins	Possible sharp, terraced or crenulated erosional margins (e.g. Lewington et al., 2020; Dewald et al., 2022).
SMC typical landforms	Presence of characteristic landforms which typically appear as distinct landform tracts, such as murtoos, murtoo-related landforms and small, irregular hummocks and ridges. Murtoo shape varies from triangular to lobate with tips typically oriented parallel to the dominant ice-flow direction and they are often associated with small-scale ridges and erosional escarpments (MREs) potentially denoting direction of local meltwater drainage (Ojala et al., 2021). SMC characteristic landforms are usually low relief (<4–5 m) and share similar dimensions (roughly 30–100 m in length and width), although small-scale ridges within hummock tracts and murtoo-related (or "oblique-parallel") ridges and escarpments tend to be narrower and longer. For detailed landform summaries and dimensions, see Ojala et al. (2021) and Vérité et al. (2024a).
Density of landforms	When margins are unclear, the density of landforms is considered alongside other criteria. In practice, this means excluding any sporadic, typically texturally smoother landforms scattered outside of the identifiable landform tracts.
Branches	SMCs with branching segments have their branches digitized individually if one or more of the following is true: notable differences in a) geomorphology, b) orientation or c) dimensions occur between segments. If present-day lakes cover significant parts of the SMC in a way that makes it difficult to determine its connectivity, the segments are digitized as individual polygons.
Lakes	Gaps in SMCs caused by present-day lakes are ignored if the SMC is interpreted to continue through the lake basin. Interpretation is based on attributes such as SMC width, orientation and geomorphology and supported by various complementary datasets detailed in Section 3.1.
Complex areas	When several SMCs are interpreted to overlap and show no clear boundaries, the entire area is collectively digitized as a "meltwater complex" instead to avoid over-estimating individual SMC dimensions. See Fig. 1B, for example.

and hummocky routes by Ahokangas et al. (2021) are included in the mapped SMCs.

Mapping and data interpretation was supported by the following complementary datasets: The Finnish Glacial Features Database (GFD) of the Geological Survey of Finland (2021) was used to assess the relationship between SMCs and other glacial landforms (see Putkinen et al., 2017). The Ancient Shoreline Database of the Geological Survey of Finland (2013) was used to locate supra-aquatic areas and calculate relative proglacial water depth (see Ojala et al., 2013). In addition, vectorized data of the Superficial deposits of Finland (scales 1:200000 and 1:1000000) by the Geological Survey of Finland (2010, 2016) were used to assist in SMC delineation and data visualization. SMCs were manually vectorized as polygons using Geographic Information System (GIS) and a set of criteria was established to assist in systematic mapping practices (Table 1). The mapping was conducted at multiple scales (1:2000–1:10000) and over multiple rounds of examinations using a semi-transparent DEM overlain on top of the hillshade.

To study regional variations in SMC characteristics, the resulting dataset was divided into four sub-regions (see Fig. 4). The division is supported by earlier literature and major geomorphological and geological differences between the areas. These sub-regions are referred to as the W and E sub-lobe of the FLDIL lobe (division marked by the Suonenjoki–Punkaharju esker; Palmu et al., 2021), and the SE and NW trunk divided by the hypothesized ice-marginal position along the Suomenselkä (Ahokangas and Mäkinen, 2014).

3.2. Morphometric analysis

The morphometric analysis consisted of measurements of length (l_p and l_n), average width (w_p), and spacing (s) (Fig. 3). The method was adopted and modified for the present study purpose from Storrar et al. (2014) and Frydrych et al. (2025). Polygon centerline length (l_p) was measured in two ways. First, when branches were digitized individually, (l_p) was calculated for each individual polygon centerline. Second, if the polygon had multiple centerlines, the length of the longest line was measured. The average polygon width (w_p) was measured by generating transects perpendicular to the centerlines at 250–500 m intervals. The centerlines were further grouped into a network dataset to capture more extensive continuations of SMCs. Grouping was made by digitizing the gaps between SMC centerlines based on their overall proximity and similar orientation. The longest line within each network was measured and expressed as (l_n). Finally, spacing (s) was measured by creating transects approximately 5 km apart across the FLDIL. The transects were first generated as straight lines perpendicular to a centerline running across the study area and subsequently adjusted and smoothed to conform to the lobate shape. Available ice sheet retreat isochrons (Stroeven et al., 2016), to which eskers and SMCs in the study area generally run perpendicular to (cf. Ahokangas et al., 2021), were used as guidelines during transect creation but could not be used to calculate spacing as such due to their sparseness. The spacing between adjacent SMCs was measured using a modified (l_p) dataset which included only the longest line of each polygon to avoid overestimating the spacing due to some SMCs having multiple centerlines.

3.3. Classifying SMC relief and SMC–esker associations

The spatial distribution of SMC relief type (see Peterson and Johnson, 2018) was mapped by assessing their cross-sectional profiles in conjunction with the DEM and the complementary datasets. Several parts of the study area are dominated by present-day lakes and bedrock exposures and the glacial overburden is generally thin and unevenly distributed (see Fig. 2A). Consequently, each SMC was assigned into one of four classes: negative-relief (Re1), positive-relief (Re2), bedrock-controlled relief (Re3) or indistinct relief (Re4) (Table 2). If the SMC had different relief types along its length, it was split into segments and divided into different classes accordingly.

The GFD (Putkinen et al., 2017) was used to identify esker ridges and assess their association with the presently mapped SMCs. Combining SMC–esker associations described in previous studies (Lewington et al., 2020; Ahokangas et al., 2021; Ojala et al., 2022; Dewald et al., 2022), each SMC was classified into one of five classes: inset esker (Es1), transitions to esker (Es2), connects to esker (Es3), cross-cut by esker (Es4), or no direct connection (Es5) (Table 2). If an SMC was associated with multiple eskers, a class Es1 or Es2 relationship was treated as the primary class and any additional relationships were recorded separately. Both of the classified datasets are presented in full in the supplementary material (Fig.S1).

4. Results

4.1. Spatial distribution of SMCs in the Finnish Lake District Ice Lobe

358 individual SMCs were digitized and cover approximately 7.4% of the FLDIL area (Fig. 4A). 213 of the features are located in the lobe and 145 in the trunk. A total of 459 centerlines were digitized within the mapped SMCs which were further combined into 156 SMC networks. Altogether, 18 SMCs were classified as meltwater complexes. The complexes in the lobe ($n = 14$) and SE trunk are either located proximal to the II Salpausselkä, or occur in association with ice lobe margins and rugged terrain, such as those distal to the Konnevesi and Toivakka regions (Fig. 8C) and east of Lake Päijänne. In the NW trunk, two complexes are found in association with an ice-flow zone margin. One occurs

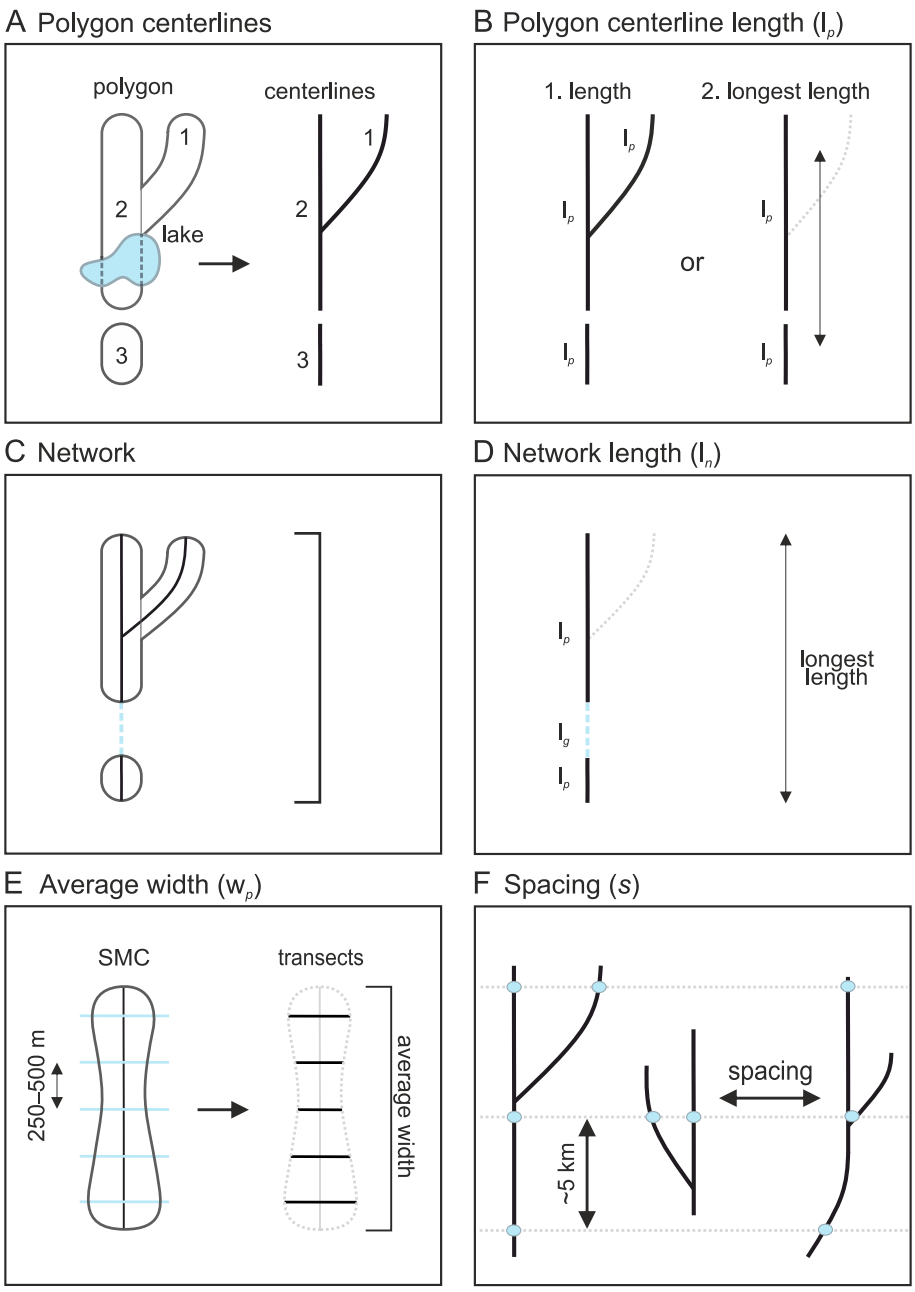

Fig. 3. Summary of the methods and workflow used to calculate SMC morphometrics. A) SMCs were digitized as individual polygons and centerlines were generated within them (1–3). B) Length of SMC centerlines (l_p) was measured. If the SMC had multiple centerlines, only the longest line was measured. C) SMC networks were created from (l_p) data. Gaps between SMCs were digitized (dashed line). D) The length of the longest line in each SMC network (l_n) was measured (l_g = gap length). E) Average width of each SMC (w_p) was calculated. F) Spacing (s) of adjacent SMCs was measured by using the longest centerline of each polygon in the (l_p) dataset. The methods are modified after Frydrych et al. (2025) and Storrar et al. (2014).

in the coastal area within the hypothesized interstream zone (cf. Ahokangas and Mäkinen, 2014).

SMCs tend to cluster distal to topographic highs, major lake basins, within rugged areas and within active ice lobe marginal zones (Fig. 4B). SMCs in the W sub-lobe have a primary orientation toward the II Salpausselkä, although many shorter SMCs are locally oriented toward longer ones. The densest SMC clusters in the region are found distal to the Toivakka–Konnevesi region, distal to lake Puula, and proximal to the bedrock exposure dominated zone up-ice from the II Salpausselkä. In the E sub-lobe, SMCs are sparse along the FLDIL–ONKIL margin aside from the cluster of SMCs oriented toward the Jaamankangas Interlobate Complex. Three distinct clusters of SMCs occur within a longitudinal band aligned with the Suonenjoki–Punkaharju esker. Of these, the Suonenjoki cluster stands out with a sharply diverging orientation toward the sub-lobe marginal zone. No SMCs were identified in the central part of the E sub-lobe where some of the major lake basins are located and where several SMCs seemingly have their onset points. SMCs in the FLDIL trunk are generally sparser along the FLDIL–MOIN margin to the east and denser along the FLDIL–NJIL margin to the west. In the NW trunk, the orientation and geometry of the SMC cluster in the coastal area of Bothnian Bay differs from the rest of the region and is connected to an esker which continues within the NJIL. In the SE trunk, SMCs cluster to the western side of the region where the topography is more variable, and the densest cluster of SMCs occurs at the onset point of the FLDIL lobe distal to Lake Keitele.

Table 2
Criteria used when classifying SMCs based on their dominant relief type and their association with eskers. Examples of different types of SMC relief and esker associations identifiable in the FLDIL area are presented in Fig. 1.

SMC relief type		SMC–esker association	
Class	**Description**	**Class**	**Description**
Re1	SMC cross-profile is negative (i.e. valley-like), with variations in width, depth and symmetricity of the valley walls (e.g. Peterson and Johnson, 2018).	Es1	Over half of the length of the SMC contains an esker (esker >50% of centerline length). Alternatively, an esker may be fully contained within an SMC regardless of its length.
Re2	SMC cross-profile is positive (i.e. ridge-like) with variations in its height (e.g. Peterson and Johnson, 2018).	Es2	SMC transitions into an esker down-ice along its length (esker <50% of centerline length) or it transitions into an esker directly from its down-ice end.
Re3	SMC cross-profile is mainly dictated by exposed or thinly covered bedrock surfaces, i.e. it has bedrock-controlled relief.	Es3	SMC is oriented toward and/or connects to an esker from its down-ice end. If an SMC has murtoos and related meltwater landforms, their orientation is used to denote orientation of meltwater flow (see Ojala et al., 2022).
Re4	SMC cross-profile is relatively flat without a dominant valley-like or ridge-like appearance, i.e. it has an indistinct relief. SMCs which have one or both of their margins concealed by lakes to an extent which makes it difficult to measure the relief accurately are also classified into this class.	Es4	SMC is cross-cut by an esker with a divergent orientation.
		Es5	SMC has no clear association with an esker.

4.2. Morphometric characteristics of SMCs

4.2.1. Length of SMCs (l_p) and SMC networks (l_n)

The statistical distribution of SMC length is unimodal and positively skewed for both the individual SMCs and SMC networks (Fig. 5A–B). Mean lengths in the datasets are 11.2 km and 18.4 km and median lengths are 7.5 km and 9.7 km, respectively. SMCs between 5 and 6 km in length are the most frequent in both datasets. For individual centerlines, SMCs exceeding 20 km make up 11.5% of the dataset, with only a few ($N = 4$) values exceeding 55 km. SMCs over 20 km in length make up 28.9% of the network dataset, of which 10 exceed 55 km. Overall, the standard deviation is high for both datasets across the FLDIL, and the median value is likely a better representative than the mean considering the skewness of the data.

Spatial differences arise when comparing statistics between the four sub-regions (Table 3). The median lengths for each sub-region do not significantly differ from the median lengths for the entire FLDIL. However, standard deviation of SMC length is relatively higher in the W sub-lobe and in the NW trunk, especially in the network dataset. The W sub-lobe has the highest mean and median values for both length measurements. The four longest SMCs (≥55 km) in the study area are located in the Pieksämäki drumlin field. The measured lengths in the E sub-lobe are shorter on average in both length datasets, and the longest feature of 42 km (l_p) in the region belongs to the Suonenjoki SMC cluster. Within the FLDIL trunk, SMCs located in the NW average longer than those in the SE.

4.2.2. Average width (w_p)

The average widths of SMCs (w_p) exhibit less variation (SD = 0.58) than their lengths across the study area (Fig. 5C). More than half (55.0%) of the data is distributed between 0.4 km and 1 km. Based on both mean and median values, the average width of SMCs is ~1.0 km. Only 6.7% of the SMCs have an average width larger than 2.0 km. It is, however, notable that out of the features exceeding 2.0 km, 12 have been classified as meltwater complexes, so some of these higher values do not necessarily represent actual, individual SMC widths. The areas classified as meltwater complexes are 2.6 km wide on average and their width varies from 1.0 to 4.4 km.

No notable differences in average width occur between the sub-regions (Table 3). However, there is variation in the spatial distribution of narrower and wider SMCs within the sub-regions. In the FLDIL lobe, the relatively wider (≥1.40 km) SMCs are mostly located within the Pieksämäki drumlin field or in the Suonenjoki SMC cluster. In the FLDIL trunk, the frequency of features ≥1.40 km increases toward the Bothnian Bay, and narrower features (≤1 km) are notably most frequent at the SE end where the trunk joins the lobate part.

A visual inspection of the data suggested that longer SMCs tended to be wider and shorter ones tended to be narrower. When plotted together, the data displays a non-uniform distribution with several outliers affecting the spread of the values, even with areas classified as meltwater complexes omitted (Fig. 5D). A statistically significant relationship was found ($p < 0.001$) when performing a two-tailed test for both Pearson's ($r = 0.329$) and Spearman's correlation ($r_s = 0.430$), indicating a weak to moderate positive correlation between the measured attributes.

4.2.3. Spacing (s)

The resulting spacing (s) dataset ($N = 633$) was trimmed by removing specified percentages of the extremely small (Min = 0.04 km) and large (Max = 185.7 km) values. This was done to better represent the lateral spacing between adjacent SMCs as the smallest values resulted from the confluence and divergence points between conjoined SMCs, and the largest values resulted from large lake basins or extreme gaps between SMCs along certain transects where SMCs were very sparse or non-existing. The data was trimmed by excluding measurements below the 5th quartile (1.2 km) and above the 80th quartile (16.2 km), which was found to effectively capture the lateral spacing within clusters of SMCs without losing relevant information (Fig. 6B–C). Unsymmetrical trimming was favored as the dataset has a higher frequency of smaller values.

The trimmed dataset ($N = 475$) has a positively skewed unimodal distribution (Fig. 6A). The mean spacing is 6.6 km and the median spacing is 5.5 km. Spacing falls most frequently between 2 and 4 km (26.7%). SD is smaller than the mean, indicating that SMCs within clusters tend to be evenly spaced. When comparing sub-regions (Table 3), mean and median spacing values appear slightly smaller than the overall average of the entire study area. The E sub-lobe and the SE trunk have smaller than average spacing according to mean, and SD is highest in the E sub-lobe and in the NW trunk.

4.3. SMC relief and geomorphology

4.3.1. Spatial distribution of SMC relief types

The predominance of different SMC relief types (Re1–4) varies across the study area (Fig. 7A–B). The dominant relief type in the W sub-lobe (39.9%) and in the SE trunk (55.0%) is negative (Re1). Negative SMCs commonly occur where till cover is sufficient for incision, such as in the Pieksämäki and Keitele drumlin fields. However, where till cover and topography are variable, many negative segments are in part associated with bedrock depressions. This is particularly apparent south of Lake Puula, where SMCs appear to be partly incised in till and partly following a major shear zone (Fig. 8A). Positive (Re2) SMC segments in the W sub-lobe and in the SE trunk regions are associated with reworked drumlin tails forming hummocky or murtoo tracts (Fig. 8B) or coincide with lower-lying areas and lack distinct margins. In the E sub-lobe, the number of positive and negative SMCs is nearly equal. Positive SMCs (29.1%) occur proximal to the II Salpausselkä and in connection to the FLDIL–ONKIL margin where hummocky moraine is present, while negative SMCs (30.3%) mainly occur in the lower lying terrain proximal

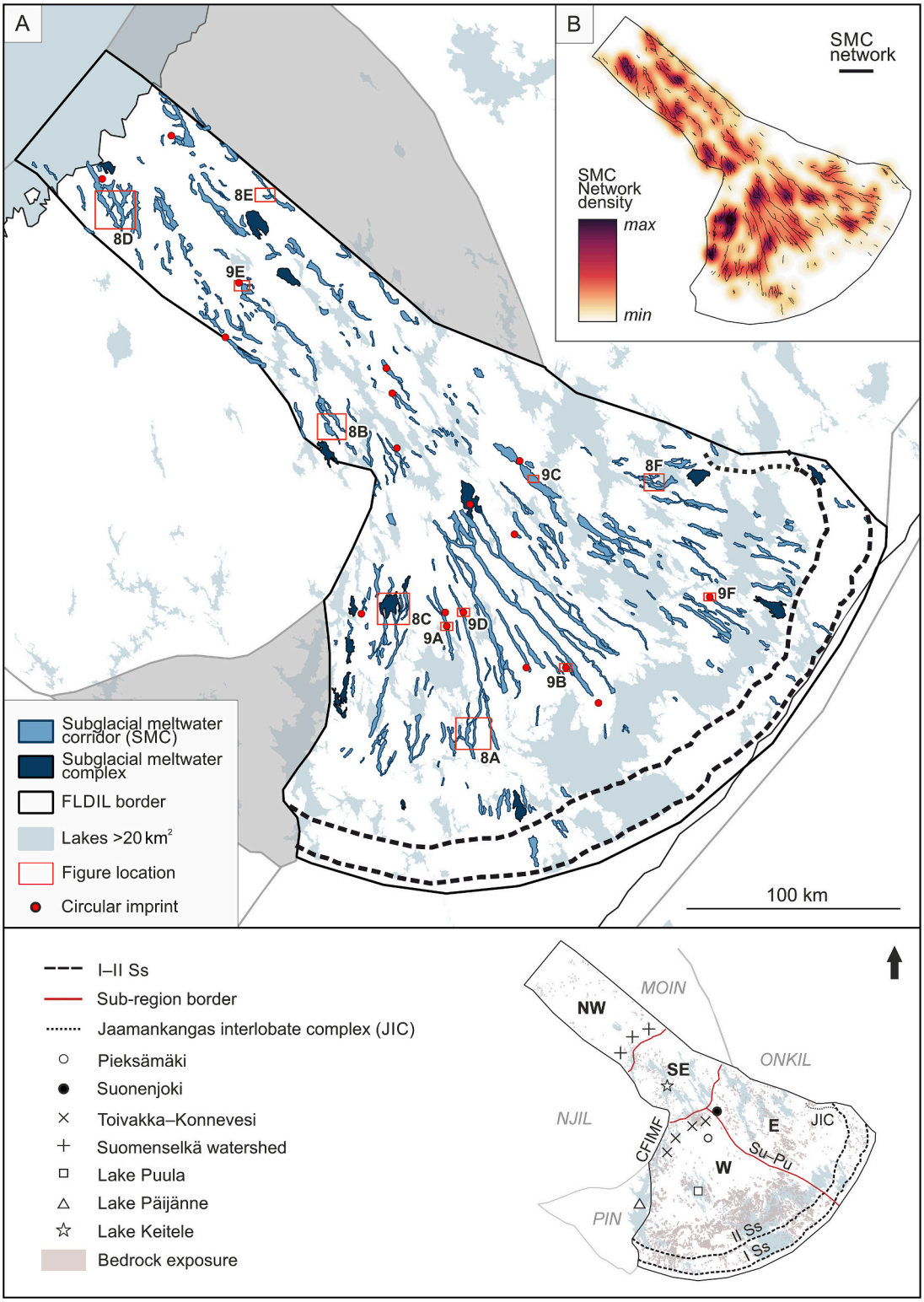

Fig. 4. A) Digitized SMC polygon data showing the spatial distribution and orientation of SMCs within the FLDIL. Locations of circular imprints (see Section 4.3.2.) and examples presented in Figs. 8 and 9 are included. B) Heatmap (Kernel density estimation, 15 km radius) depicting SMC network density based on points created at transect intersections (see Fig. 3F). The legend below contains key locations, sub-region divisions and bedrock exposures. See Fig. 2. for further explanations of abbreviations.

to the II Salpausselkä. In areas where till cover is irregular and topography is variable, SMCs overall tend to fall within the bedrock-controlled (Re3) category. Murtoos and related landforms are especially common within the bedrock-controlled and positive SMCs in the E sub-lobe (Fig. 8F) and in the Konnevesi meltwater complex area.

In contrast to the other sub-regions, the NW trunk is dominated by positive-relief SMCs (55.7%) with occasional negative and indistinct segments. The positive SMCs are found within the extensive hummocky and ribbed moraine fields flanking the streamlined terrain and appear notably wider than the mostly negative SMCs in the SE trunk. On the

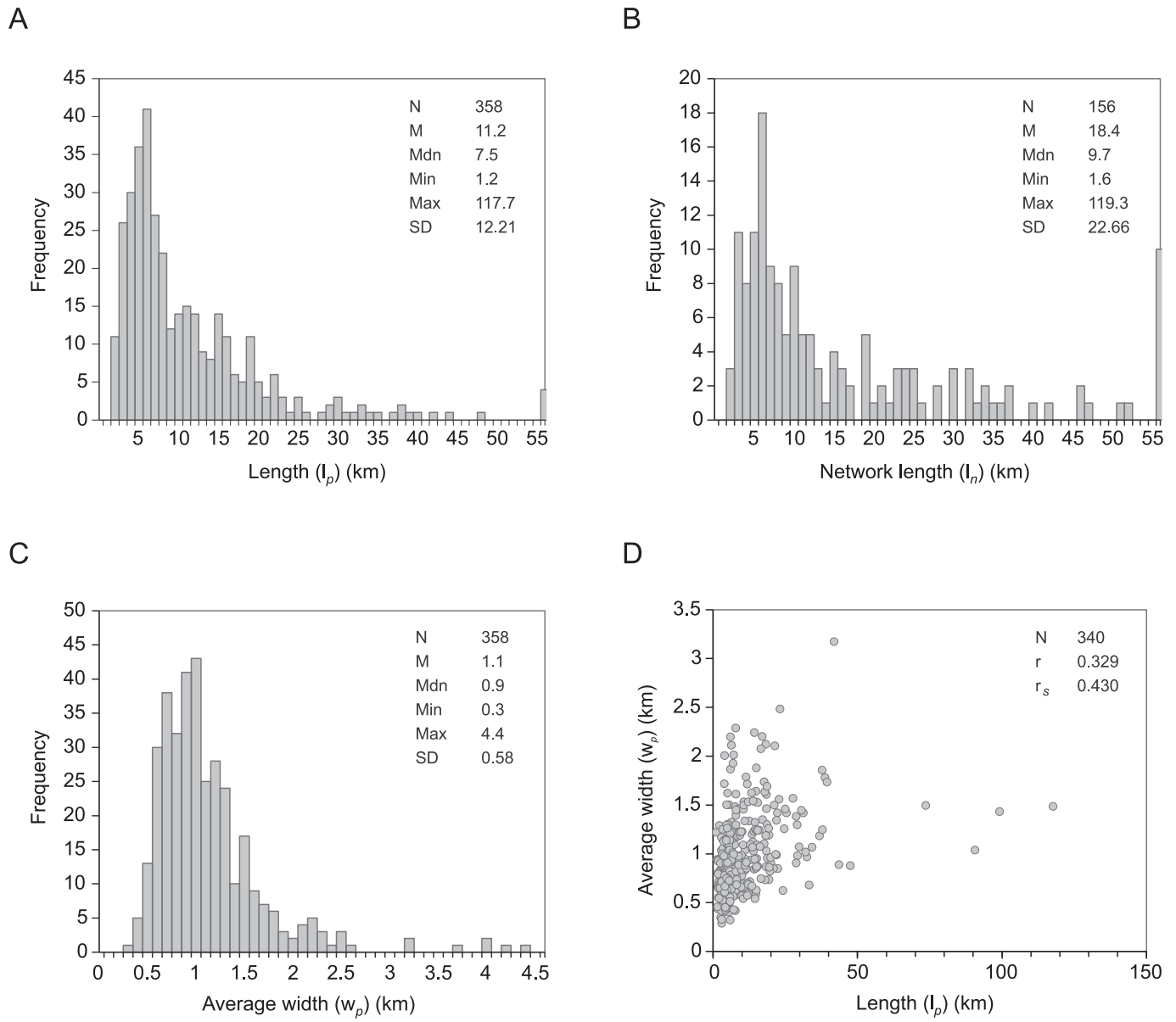

Fig. 5. A) Frequency distribution of the lengths of individual SMC centerlines (l_p). B) Frequency distribution of the lengths of the longest continuous line in each SMC network (l_n). C) Frequency distribution of the average SMC width (w_p). D) Relationship between SMC length (l_p) and average SMC width (w_p) indicating a tendency for longer SMCs to be wider. Areas classified as meltwater complexes have been omitted from the comparison. Notice that the final column of each length distribution histogram combines all values equal or larger than 55 km.

western side there is a tendency for positive SMCs to occur further inland, while negative SMCs are found closer to the FLDIL–NJIL margin (Fig. 8D). This pattern is not found along the FLDIL–MOIN margin to the east, where SMCs predominantly have an indistinct or positive relief (Fig. 8E). Indistinct (Re4) SMCs in the FLDIL region are mainly tied to lake basins partly or fully obscuring SMC margins. However, when this is not the case, they are found on even terrain and commonly exist as shorter segments within otherwise positive or negative-relief SMCs.

4.3.2. Geomorphological characteristics of SMCs

Negative-relief SMC margins range from smooth and indistinct to sharp and erosional, while some segments are partly or mostly bedrock-confined. In the Pieksämäki drumlin field and distal to Lake Puula, negative SMCs clearly incised in sediment typically range from 5 to 20 m in depth, whereas those in the Toivakka region and in the E sub-lobe appear shallower and lack distinct margins. SMCs with crenulated margins are primarily found clustered distal to the Toivakka–Konnevesi region and Lake Puula (Fig. 8A). Negative SMCs in the SE trunk generally range from a few meters to approximately 10 m in depth. In the NW trunk, negative SMCs tend to be <5 m deep. Although SMCs in the region are generally less linear and lack distinct margins, erosional escarpments (see Ojala et al., 2021) are particularly common and in many instances partially form the margins of the SMCs (Fig. 8E).

Overall, landforms within SMCs are well-preserved with little to weak evidence of subsequent overriding by ice. However, SMC margins in places exhibit streamlined surfaces (Fig. 9C). These occur more commonly in the FLDIL lobe and are located in topographically higher areas and closer to the bedrock exposure dominated region proximal to the II Salpausselkä. Some instances of fluted surfaces were also found within the lowland region of the Pieksämäki drumlin field on landforms interpreted as reworked drumlins, which notably exhibit ribbed-like forms (Fig. 9D) and are often found within or in proximity of murtoo fields.

Several circular imprints ($N = 18$) akin to the paleo-blister described

Table 3
Summary of the morphometric statistics presented in this study. Note that when measuring spacing (*s*) within each sub-region, the transects left between SMC centerlines and sub-region borders were removed, so the total number of measurements ($N = 449$) for the sub-regions is less than that of the entire study area.

Region	Parameter (km)	N	Mean	Median	Min	Max	SD
FLDIL total	length (l_p)	358	11.2	7.5	1.2	117.7	12.21
	width (w_p)	358	1.1	0.9	0.3	4.4	0.58
	network length (l_n)	156	18.4	9.7	1.6	119.3	22.66
	spacing (*s*)	475	6.6	5.5	–	–	4.04
W sub-lobe	length (l_p)	115	14.8	10.0	1.9	117.7	17.93
	width (w_p)	115	1.1	0.9	0.3	4.0	0.60
	network length (l_n)	47	23.8	11.2	2.5	119.3	30.00
	spacing (*s*)	207	6.2	5.5	1.2	14.8	3.41
E sub-lobe	length (l_p)	98	10.2	6.5	1.6	42.0	7.90
	width (w_p)	98	1.1	1.0	0.4	4.4	0.60
	network length (l_n)	42	18.4	9.2	1.6	102.2	19.69
	spacing (*s*)	95	5.8	4.3	1.2	14.8	4.12
SE trunk	length (l_p)	61	8.2	5.9	1.2	24.2	5.87
	width (w_p)	61	0.9	0.8	0.4	2.1	0.40
	network length (l_n)	34	11.5	7.4	2.1	55.5	10.78
	spacing (*s*)	49	5.9	5.5	1.3	13.7	3.10
NW trunk	length (l_p)	84	9.7	6.6	1.5	38.8	7.75
	width (w_p)	84	1.2	1.0	0.3	3.9	0.60
	network length (l_n)	33	17.6	10.0	1.6	103.7	21.03
	Spacing (*s*)	98	6.3	5.1	1.2	14.8	3.92

by Mäkinen et al. (2023b) were identified within the SMCs during the classification process (See Fig. 4A). The depressions range from c. 0.1 to 4.5 km in diameter. Majority of them have multiple small channels radiating from the circular depression (Fig. 9A), although a few have a single, larger down-ice channel (Fig. 9B). The depressions tend to occur on the lee sides of drumlins, distal to topographic highs and within rugged regions of the bed and often coincide with murtoo fields (Fig. 9F). A few circular depressions ($N = 3$) were also identified in the NW trunk on flat terrain, although their appearance is considerably less distinct compared to those described in the FLDIL lobe (Fig. 9E).

4.4. SMC–esker associations

Differences in SMC–esker associations (Es1–Es5) are apparent across the study area. In addition to the primary classification, 18 SMCs were assigned a secondary classification due to multiple esker associations. Of these, 17 are located in the FLDIL lobe, of which 14 are classified as a cross-cutting relationship (Es4). SMCs with a secondary classification are mostly located in the vicinity of ice-marginal zones, such as proximal to II Salpausselkä, in the Toivakka region, or within the Suonenjoki SMC cluster.

Nearly half of the SMCs in the W sub-lobe (Fig. 7C) either have an inset esker (Es1; 21.7%) or transition to an esker down-ice (Es2; 25.2%). SMCs with inset eskers are particularly concentrated within the Pieksämäki region and are flanked by the generally shorter and narrower Es2 SMCs or joined by Es3 SMCs (Fig. 10A). SMCs which either connect to an esker (Es3) or are cross-cut by an esker (Es4) in the W sub-lobe occur most commonly within rugged areas of the bed and closer to the II Salpausselkä (Fig. 10B). In the E sub-lobe, SMCs with an Es1 or Es2 type association are less frequent and mostly occur 65 km up-ice from the II Salpausselkä (Fig. 10C). Similar to the W sub-lobe, Es3 and Es4 type SMCs in the region are widespread within rugged areas of the bed where murtoo fields also frequently occur. SMCs which connect to eskers are especially common (34.7%) in the region and are associated with the sub-lobe marginal zones. Overall, SMCs without esker connection (Es5) have no apparent pattern in their distribution in the FLDIL lobe, but appear more frequently in the E sub-lobe (31.6%).

In contrast to the lobate part, Es1 and Es2 SMCs are markedly less frequent in the FLDIL trunk (Fig. 7D). Majority of the SMCs in the SE trunk have no apparent esker connection (52.5%), and SMCs which transition to eskers concentrate to the western side at the onset point of the FLDIL lobe (Fig. 10D). Es3 SMCs are the most frequent association type in the NW trunk (45.2%). SMCs with no esker connection (39.3%) commonly appear as short and isolated segments especially on the western side of the region. Aside from this, no prominent spatial patterns can be observed in the distribution of the SMC–esker association types in the region, and unlike in the FLDIL lobe, murtoo fields are found distributed more evenly across the classes.

Finally, a trend can be observed between median SMC length (l_p) and the recorded SMC–esker association. Es1 SMCs are slightly longer on average (14.3 km) compared to Es2 (12.9 km) and Es4 (12.2 km) SMCs. Es3 (6.4 km) and Es5 (5.9 km) SMCs are markedly shorter on average. This relationship is visually most pronounced within the Pieksämäki drumlin field. A general relationship can also be observed between SMC–esker associations and the dominant relief type of the SMC. When calculating the total area (km^2) of each SMC relief class within each SMC–esker association class, it became apparent that Es1 SMCs tend to mostly consist of type Re1 segments (52.2%) with other relief types constituting $\leq$20% of the total area. Conversely, a larger portion of Es3 SMCs consists of Re2 segments (46.1%).

5. Discussion

5.1. Comparison of SMC morphometrics to earlier work on subglacial meltwater routing

The densest SMC clusters occurred within rugged regions, distal to topographic highs and present-day lake basins, in connection to ice lobe marginal zones and in association with the western margin of the ice stream trunk. This large-scale spatial pattern is in agreement with the earlier mapping by Ahokangas et al. (2021). Some regional differences nevertheless occur in the rugged areas of the lobe and in the SE trunk, where the numerous short and disconnected SMRs were integrated into a more extensive drainage network in the present study. Furthermore, multiple unmapped areas east of Lake Päijänne basin were included in the present dataset as meltwater complexes. Our mapping also did not include individual meltwater channels unlike Ahokangas et al. (2021), who identified several within the center of the E sub-lobe, where SMCs and eskers are sparse. The present dataset may therefore underestimate drainage density in some regions.

The average length of SMCs in the study area according to median values was 7.5 km (mean = 11.2 km) for SMC centerlines and 9.7 km (mean = 18.4 km) for SMC networks. They also exhibited a consistent average width of approximately 1 km. The average width is comparable to those reported in Canada and Sweden (Peterson and Johnson, 2018; Lewington et al., 2020), but mean and maximum recorded lengths display high variation between the studies. This variation likely reflects differences in mapping approaches rather than meaningful variance in SMC characteristics. A comparison with Dewald et al. (2022) is similarly not straightforward due to different classification approaches. However, Dewald et al. (2022) found a tendency for SMCs associated with esker ridges to be longer than those not associated with eskers, which aligns with our findings.

Although we aimed to capture SMC continuity by integrating individual centerlines into a network dataset, SMC length is still likely underestimated in bedrock exposure and lake dominated areas, where the terrain inhibited reliable SMC delineation in the current study. One such example is the region proximal to the II Salpausselkä in the W sub-lobe, where some of the long and prominent SMCs with inset eskers probably continue further down-ice toward the II Salpausselkä (cf. Dewald et al., 2022). Postglacial deposits, widespread hummocky terrain and the lack of distinct SMC margins in the NW trunk impose

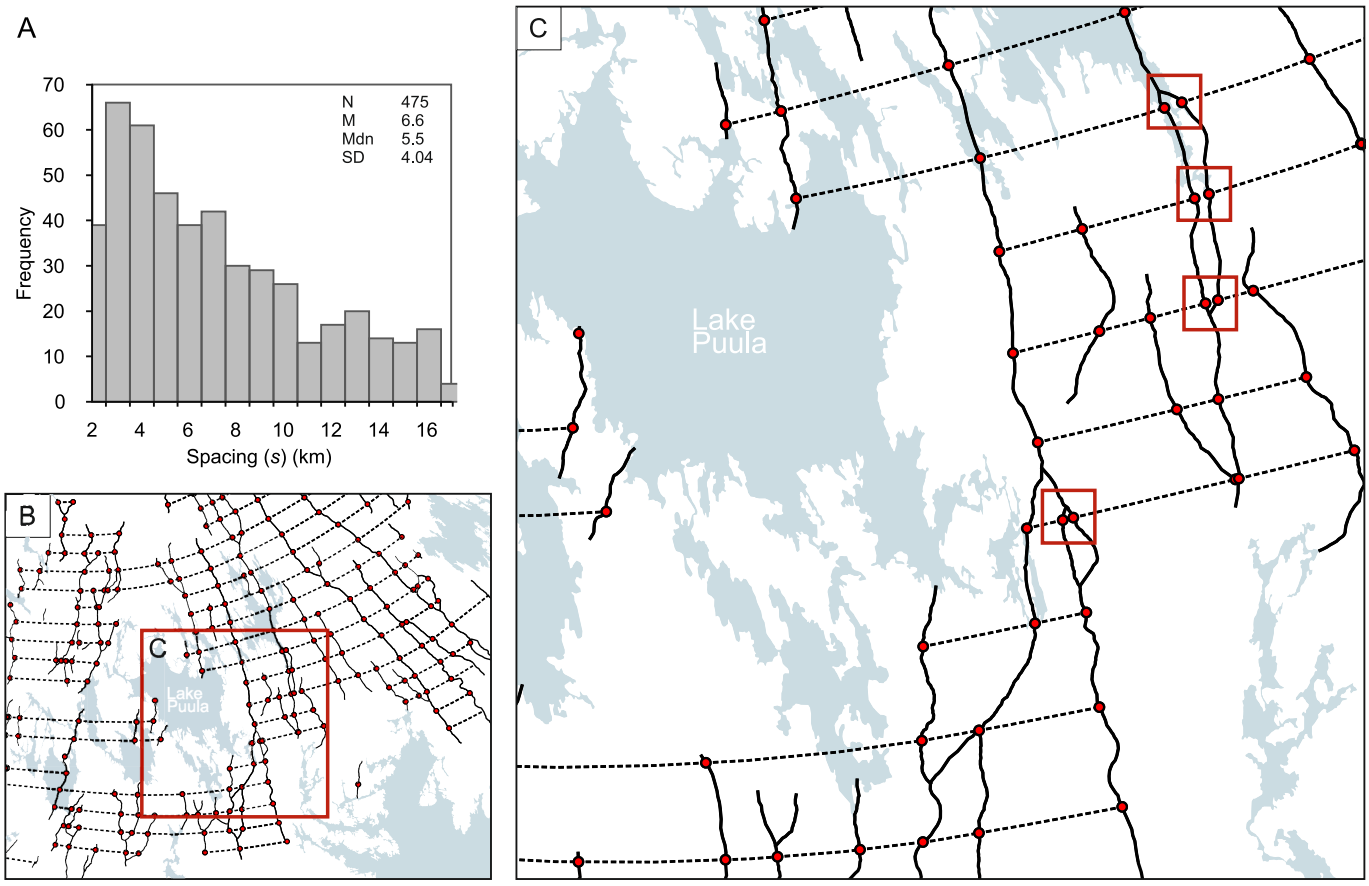

Fig. 6. A) Frequency distribution of the spacing (*s*) between SMCs across the study area. The depicted data has been trimmed by the 5th quartile and the 80th quartile. Notice that the final column of the distribution histogram combines all values equal or larger than 16 km. Visual examples of the trimmed dataset from the Lake Puula region in the W sub-lobe illustrate: B) Removal of large gaps caused either by major lakes obscuring the landscape or by the absence of SMCs altogether along certain transects, and C) Removal of smallest values resulting from intersection points of conjoining/diverging SMCs (red squares). (For interpretation of the references to colour in this figure legend, the reader is referred to the web version of this article.)

additional challenges in reliably distinguishing SMC dimensions and continuation. Although our dataset matches the general drainage patterns reported by Ahokangas et al. (2021) and Dewald et al. (2022) in the region, the actual extent of the subglacial drainage may be more widespread than what our present dataset is able to capture.

Negative SMCs have been likened to tunnel valleys due to their similar morphometry and their frequent association with eskers (Peterson and Johnson, 2018). In the southern sector of the Laurentide Ice Sheet, Livingstone and Clark (2016) identified a tendency for longer tunnel valleys to be wider (power law function, $r^2 = 0.34$). The correlation between SMC length and width in the FLDIL shows a comparable positive relationship, which contrasts the findings of Peterson and Johnson (2018), who did not identify similar correlation in the south Swedish uplands (SSU). Livingstone and Clark (2016) attributed this relationship to gradual headward extension and/or continuous flow, and proposed that the length and width of tunnel valleys formed solely by outburst floods would likely be independent of each other. The positive length–width relationship observed in the FLDIL may therefore indicate time-transgressive origin for the majority of the studied SMCs.

Subglacial conduit spacing is controlled by a combination of substrate properties, basal melt rates, the hydropotential gradient (e.g. Boulton et al., 2009; Hewitt, 2011) and supraglacial meltwater fluxes (Storrar et al., 2014) in such that lower bed transmissivity, higher supraglacial and/or basal melt rates and a steeper hydropotential gradient would result in more closely spaced eskers and tunnel valleys (Storrar et al., 2014; Livingstone et al., 2016). Although the average SMC spacing was relatively uniform across the studied sub-regions, the mean values for the E sub-lobe and the SE trunk showed slightly smaller spacing. Both of these regions are characterized by rugged terrain, which could have at least in part controlled the lower than average spacing. Although our present measurement approach does not capture spatial variations within the sub-regions, the SMC cluster distribution does also imply significant topographic control on SMC density.

Lateral spacing between adjacent SMCs in the entire FLDIL averaged 6.6 km (mean) and 5.5 km (median). Esker spacing generally ranges from less than 2 km to 35 km in literature, with results from the LIS indicating a preferred spacing of 12–15 km (Storrar et al., 2014 and references therein). The mean spacing of eskers in the FLDIL ranges from 9.7 to 12.7 km in the lobe and 14.0 to 25.0 km in the trunk (Boulton et al., 2009). Eskers are typically associated with locations of former subglacial conduits, which are generally considered to exist in lower pressure and drain water from the surrounding, wider distributed system (Röthlisberger, 1972; Hewitt, 2011). While some of the mapped SMCs could have formed within a channelized environment, a large portion of them likely formed in conditions ranging from distributed to semi-distributed as indicated by the presence of murtoos (Hepburn et al., 2024). This semi-distributed drainage signature over a larger portion of the bed would yield an overall narrower average spacing for SMCs than that of eskers, which indicates that active subglacial drainage in the FLDIL occupied roughly twice the area than what is implied by the esker distribution alone.

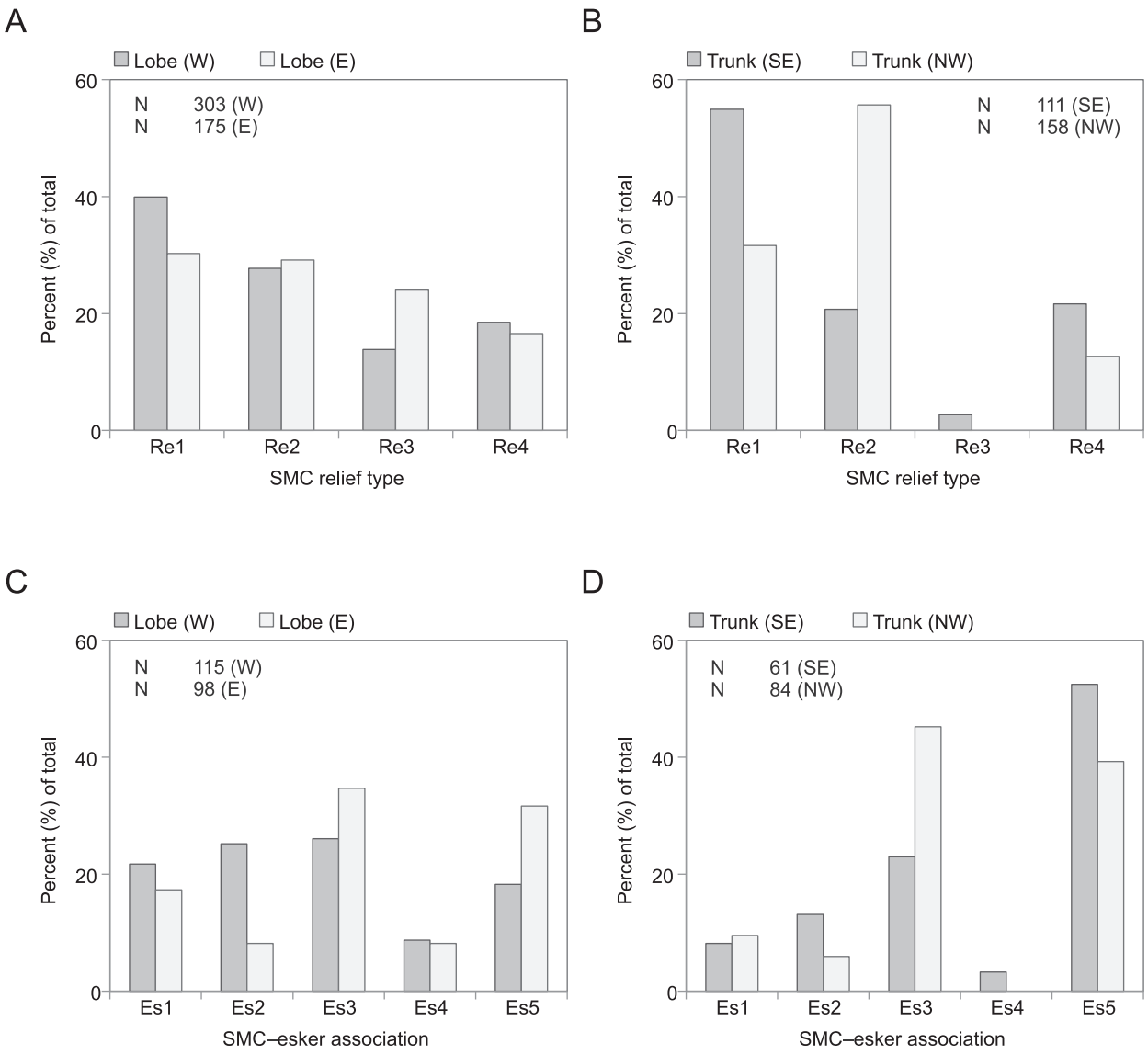

Fig. 7. Distribution of SMC relief types (Re1–4) and SMC–esker association types (Es1–5) between the sub-regions of the study area. Columns represent % of each class relative to the total number of features in each sub-region.

5.2. Geological and geomorphological controls on SMC form and distribution

In this study, we defined meltwater complexes as areas where several adjacent SMCs appear to overlap without distinguishable boundaries, and thus probably correspond to zones that experienced repeated and spatially heterogenous meltwater drainage in varying magnitudes. Lewington et al. (2020) reported that densest SMRs occurred in areas of variable topography and connected this to the fragmentation of drainage around bedrock obstacles and/or spatially distributed meltwater delivery to the bed. This relationship is well-demonstrated in the FLDIL lobe where dense SMC clusters consisting of meltwater complexes and bedrock-controlled SMCs are located within the relatively higher and rugged regions of the bed. The concentration of murtoos within these areas also supports distributed drainage conditions which would allow their widespread deposition and preservation (Ojala et al., 2022). Some meltwater complexes were also observed proximal to the II Salpausselkä, where they may be partly related to the earlier deglaciation and II Salpausselkä deposition stage prior to the onset of the Holocene.

The densest networks in the NW trunk were connected to the active ice stream and ice-flow zone margins (see Ahokangas and Mäkinen, 2014), where we also identified three meltwater complexes. Previously, Ahokangas et al. (2021) suggested that murtoo route (i.e. murtoo tract) distribution is related to increased crevassing and shear-induced melting of ice in certain environments, including the shear margins of ice streams (cf. Meyer et al., 2018) and ice-flow zones and stoss sides of topographic highs, such as the Konnevesi region. However, they also considered the role of supra- and subglacial drainage inputs in murtoo formation, which we will further discuss in the following sections.

Several SMCs within the study area followed topographic lows and elongated bedrock depressions. Their formation in formerly glaciated crystalline bedrock areas is often associated with large-scale brittle and ductile deformation zones and lithological contacts (Skyttä et al., 2015; Krabbendam and Bradwell, 2014; Ruuska et al., 2023), particularly where the zones of structural weakness align with the dominant ice-flow direction (Krabbendam et al., 2016; Skyttä et al., 2023). The ice-flow parallel strike of the bedrock in the Pieksämäki–Keitele region contributed to the formation of the drumlin fields (Glückert, 1973; Krabbendam et al., 2016) and the NW–SE-oriented fracture zones in the lobe (Lunkka and Erkkilä, 2012), where the long, mainly negative-relief SMCs with inset eskers or down-ice transition to eskers also occur. Subglacial drainage is partly controlled by subglacial topography, especially under

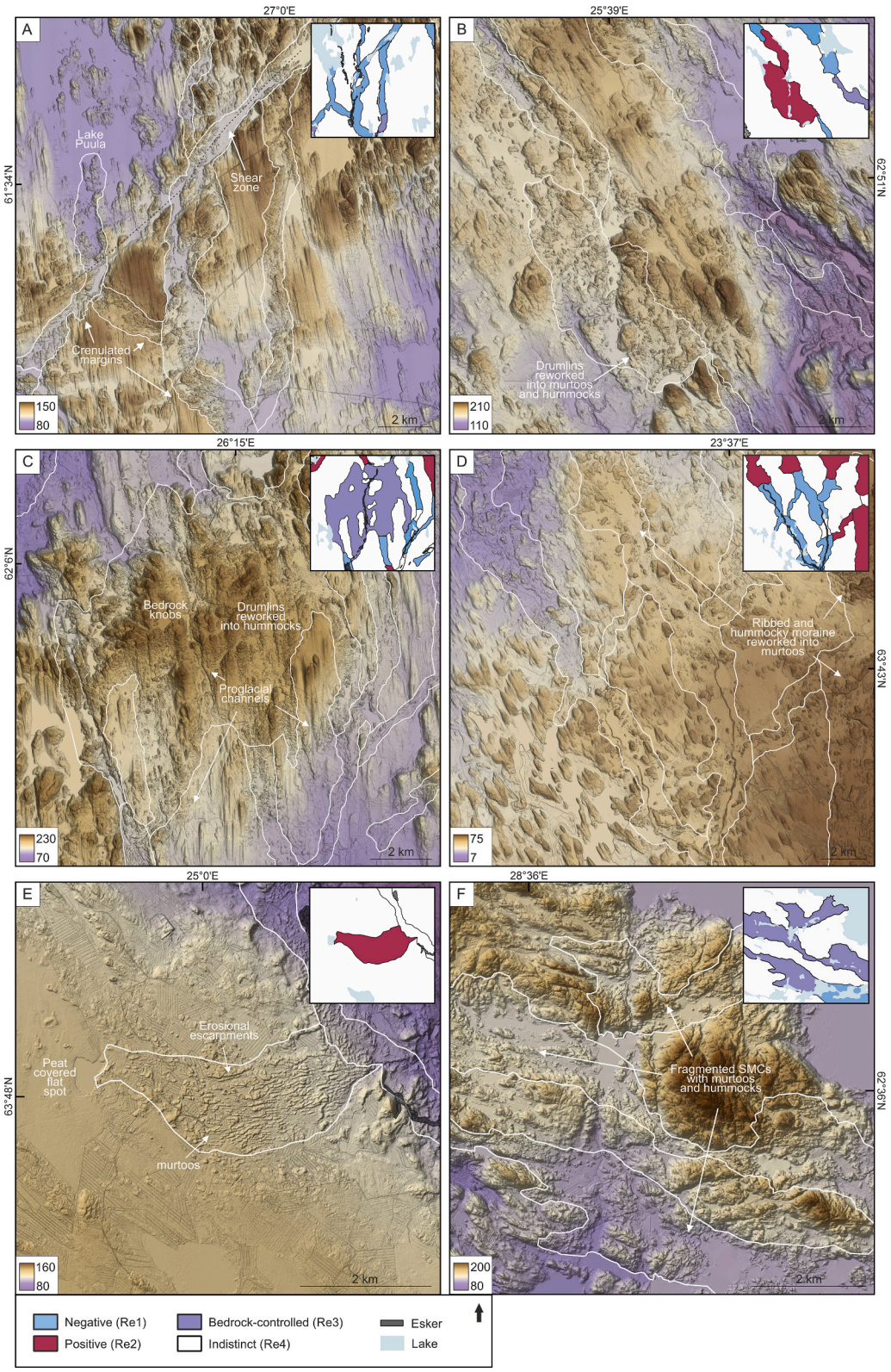

Fig. 8. A) Negative-relief (Re1) SMCs south of Lake Puula. The SMCs are partly incised in till and partly following visible bedrock depressions. The depression indicated with a dashed line is related to a major shear zone which consists of several faults. B) Positive-relief (Re2) SMC segment consisting of hummocks and murtoos formed from reworked drumlin tails. C) Mainly bedrock-controlled (Re3) relief in the Toivakka region. The area represents a meltwater complex and the relief is a mixture of bedrock knobs, incised till surfaces, reworked drumlin tails and small hummocks. Note proglacial channels cutting other landforms. D) Positive (Re2) SMCs transitioning into shallow negative (Re1) SMCs with inset eskers in the coastal region of the Bothnian Bay. Positive segments are mostly the result of ribbed and hummocky moraine being partly reworked into murtoos and murtoo-related landforms. E) Positive-relief (Re2) SMC consisting of murtoos originating from a flat, peat covered spot. The SMC connects to an indistinct (Re4) relief SMC. F) Bedrock-controlled SMCs with a fragmented appearance consisting of murtoos, hummocks and exposed bedrock surfaces. See Fig. 4A for each location. Background data: DEM (© National Land Survey of Finland).

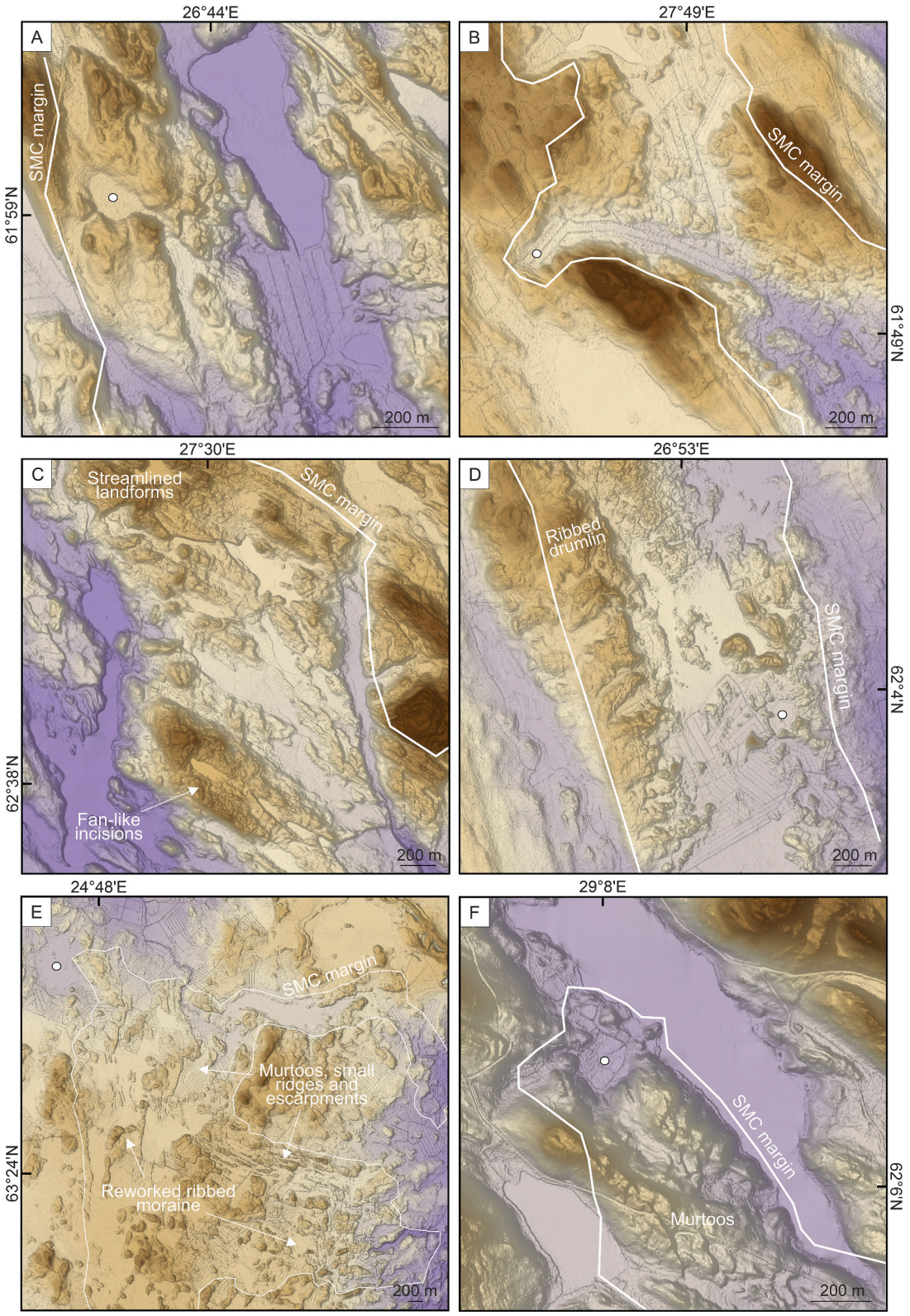

Fig. 9. Examples of features identified within the SMCs during the classification process. White dots mark the centers of circular imprints. A) Circular imprint with multiple small channels radiating from the depression located on the lee side of a drumlin. B) Circular imprint with a large down-ice channel cross-cutting a hummocky SMC. C) Section of an SMC belonging to the Suonenjoki cluster with streamlined landforms at its margins. Repeated fan-like incisions are found on the lee side of a drumlin to the south. D) Drumlin tail with a distinctly ribbed-like form within an SMC. The surface of the form is fluted. A circular imprint interpreted as a possible paleo-blister by Mäkinen et al. (2023b) is located east of the drumlin. E) An indistinct circular imprint located at the onset of an SMC with divergent branch orientations and heavily reworked ribbed moraines. F) A circular imprint located up-ice of a small murtoo field. See Fig. 4A for locations. Background data: DEM and DEM-based hillshade (© National Land Survey of Finland).

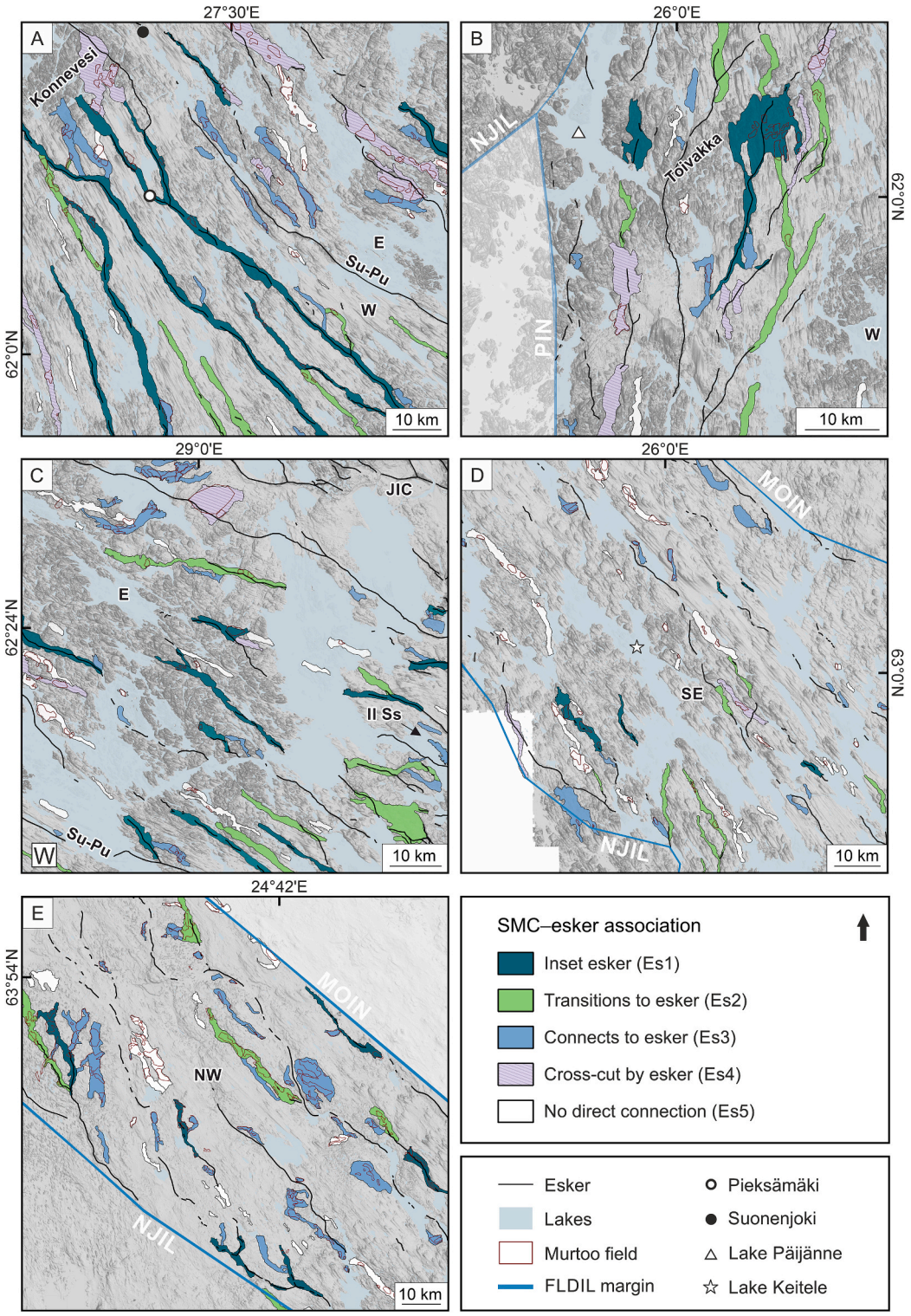

Fig. 10. Examples of SMC–esker associations across the FLDIL. A) Mainly Es1 and Es2 SMCs distal to the Konnevesi region (W sub-lobe). SMCs belonging to the Suonenjoki cluster in the E sub-lobe are mostly Es3 and Es4 type. Note the stark difference in SMC–esker associations and the prevalence of murtoo fields between the two sub-regions. B) SMC–esker associations in the Toivakka region (W sub-lobe). Several of the SMCs are classified as meltwater complexes and have a secondary cross-cutting association with an esker. C) Mainly Es1 and Es2 type SMCs proximal to the II Salpausselkä in the E sub-lobe. Es3 and Es4 type SMCs occur in connection to the Jaamankangas Interlobate Complex. D) SMC–esker associations in the SE trunk. Es1 and Es2 type SMCs are located mainly on the western side of the sub-region. E) Mainly Es3 type SMCs in the NW trunk. Note the frequency of murtoo fields in the region. Background data: DEM (© National Land Survey of Finland). Murtoo fields and eskers (polylines) provided by Ahokangas et al. (2021).

thinner ice (Shreve, 1972). Channelization is generally limited to <50 km from the ice sheet margin in western Greenland (Dow et al., 2014; Greenwood et al., 2016), and eskers are largely considered to deposit time-transgressively within the ice-marginal environment (e.g. Mäkinen, 2003). Eskers and ice-marginal glacifluvial deposits, such as those associated with the Salpausselkä ice-marginal complexes, often align with fracture- and shear zones in the hard-bed areas of southern Finland (Skyttä et al., 2015; Frydrych et al., 2025). Together, these results suggest that the underlying bedrock exerted strong control on the long-term spatial stability and organization of drainage in the FLDIL by influencing meltwater routing both within and outside of the channelized environment.

Vérité et al. (2024a) discussed the role of pre-existing landforms and their interactions with spatiotemporally varying meltwater inputs. They conceptualized a divide between i) water erosion and deposition-dominated SMCs and ii) deformation-dominated SMCs. They also suggested the prior to be more widespread, and our results agree with this notion. In general, we found truly indistinct relief (Re4) SMCs rare, and a large portion of the segments classified as such were rather related to partly or fully lake-covered sections. Some Re4 SMCs, however, could represent short-lived pathways or lesser magnitude drainage activity, which would result in indistinct morphology and inapparent esker associations. In places, postglacial deposits could also result in indistinct SMC relief, especially in the NW trunk.

The prevalence of negative-relief SMCs and bedrock exposure dominated regions in the lobe indicates considerable sediment removal. The eroded material has likely been deposited into the murtoo and hummock tracts, eskers and marginal formations (e.g. the II Salpausselkä), or deposited in present-day lakes. The extensive zone of exposed bedrock proximal to the II Salpausselkä in the W sub-lobe, however, is probably related to the earlier deglaciation and readvance stages (i.e. the Heinola deglaciation) prior to the deposition of the II Salpausselkä (Lunkka et al., 2021) rather than post-Younger Dryas meltwater activity.

In spite of negative relief being dominant overall, the NW trunk mainly contains positive SMCs (Re2) with frequent murtoos and murtoo-related landforms located within hummocky and ribbed moraine fields. Ribbed and Rogen-type moraines (see Möller, 2006) are common within the cold central areas of the FIS and originated within the transitional zone between cold- and warm-bed conditions (Sarala, 2025). Extensive ribbed and hummocky moraine fields between the glacially lineated terrain in the NW trunk are related to areas of slower ice flow (Ahokangas and Mäkinen, 2014). Vérité et al. (2022) previously demonstrated how ribbed bedforms are transformed into murtoos through repeated episodes of erosion, deposition and deformation resulting from periodic flooding along meltwater corridors. The SMC relief and landform assemblages presented here could therefore indicate deformation-dominated processes within the NW trunk (Vérité et al., 2024a).

Extensive ribbed moraine fields are absent elsewhere in the study area, where positive SMC segments were regularly associated with heavily reworked drumlins and, in places, hummocky moraine terrain. However, instances of ribbed bedforms, including “ribbed” drumlins (see Dunlop and Clark, 2006) were found restricted within SMCs (Fig. 9D). Recent kinematic and conceptual models (Vérité et al., 2024b) and examples from modern and paleo-ice sheet beds (Sergienko and Hindmarsh, 2013; Stokes et al., 2016) describe the role of meltwater pressure fluctuation driven instabilities in bed deformation and ribbed bedform genesis. Local variations in sediment pore water pressure and ice-bed coupling along the margins of drainage corridors could result in “transitional” ribbed bedforms (Vérité et al., 2024a-b), which might explain the occurrence of these isolated landforms along SMCs.

5.3. SMC–esker associations reflecting spatiotemporally varying drainage modes

The subglacial hydrological system is often conceptualized through independent drainage modes (e.g. Fountain and Walder, 1998), although in reality, its structure and hydraulic connectivity changes in response to meltwater input, ice sheet geometry and bed topography (Schoof, 2010; Hoffman et al., 2016; Davison et al., 2019; Schoof, 2023). We sought to examine how the interactions between SMCs and eskers vary across the FLDIL by dividing their interaction types into five classes (Es1–Es5; see Table 2 for a summary).

Our results from the W sub-lobe revealed SMCs with inset eskers (Es1) which form continuous, >100 km long and primarily negative pathways. These record the final, geomorphic imprint of spatially stable subglacial meltwater flow. SMCs which transition to eskers down-ice (Es2) often had comparable relief but tended to be shorter and narrower. The spatial transition toward conduits occurring along these pathways indicates shifts in drainage conditions, which likely result from changes in meltwater input or ice sheet geometry. Larger quantities of meltwater and a steeper hydropotential gradient near the ice margin can reduce the size of subglacial meltwater catchment basins causing smaller channels to open up between larger ones (Hewitt, 2011). This pattern is similar to the morphometric and spatial relationship between SMCs in the Pieksämäki region (Fig. 10A), where the simultaneous termination of the smaller corridors may indicate decreasing meltwater supply or drainage reorganization toward the more efficient major SMCs during margin retreat.

Theory suggests that in a steady-state system, subglacial water flows from higher pressure regions toward lower pressure, channelized systems (Greenwood et al., 2016; Hewitt, 2011). Lewington et al. (2020) described spatial interactions between conduits and the surrounding, connected distributed system (variable pressure axis, see Davison et al., 2019), where fluctuations in water pressure determine whether subglacial meltwater flow is drawn into a conduit or spreads laterally during over-pressurization events. Some of our Es1 and Es2 SMCs may result from similar, repeated interactions between the central conduit (esker) and the surrounding, hydraulically connected distributed drainage (the meltwater corridor), resulting in mainly erosional corridors containing hummocks, eskers and glacifluvial deposits (cf. Lewington et al., 2020).

Ojala et al. (2022) described an SMC within the Baltic Sea Ice Lobe which they interpreted to record development from distributed or semi-distributed drainage (i.e. murtoos) to efficient channelized drainage (esker). SMCs which connect to eskers (Es3) were especially frequent in the E sub-lobe and the NW trunk and displayed mainly positive or bedrock-controlled relief. These types of SMCs were typically shorter and, importantly, frequently consisted of murtoos and murtoo-related landforms (Ojala et al., 2021). SMCs cross-cut by eskers (Es4) in the lobe likewise frequently contained murtoos and had similar relief. The cross-cutting relationship indicates that these SMCs formed further away from the ice margin and were later superimposed as the hydraulic gradient adjusted during deglaciation. Consequently, we interpret SMCs with Es3 and Es4 type associations to primarily record distributed to semi-distributed drainage, which routed subglacial meltwater toward lower pressure conduits, major SMCs, sub-lobe margins and ice stream marginal zones.

Extensive lake coverage, limited to non-existent sediment cover and postglacial deposits in places cause uncertainties in SMC length and continuity. Since our present classification scheme depended on the relationship between SMC and esker length, these topographical constraints naturally also affect the division between Es1 and Es2 associations. The same applies to SMCs classified as having no apparent esker connection (Es5), and the current results may therefore overestimate the number of SMCs in this class. Even so, our results indicate that, when used along other parameters, SMC–esker associations could reflect prevailing drainage configurations and reorganization on a regional-scale and can therefore provide new information on drainage

evolution during deglaciation.

5.4. The role of surface meltwater inputs and subglacial ponding in SMC formation

In previous studies in Finland, SMCs and murtoo fields have mainly been proposed to form by (i) supraglacially derived meltwater via moulin/crevasse-to-bed connections (Mäkinen et al., 2023b), (ii) periodic drainage of subglacial lakes (Ahokangas et al., 2021), and iii) shear-induced melting in certain settings, which were discussed in detail by Ahokangas et al. (2021). Although potential paleo-subglacial lake locations (e.g. Kajuutti et al., 2016; Tuunainen, 2018) and meltwater blister imprints (Mäkinen et al., 2023b) have been proposed beneath the Finnish sector of the FIS, geomorphological evidence examining their distribution remains limited. In light of the evidence obtained in this study, we discuss here the potential role of supra- and subglacial meltwater inputs in SMC formation.

A significant portion of meltwater in the contemporary Greenland Ice Sheet is routed to its bed via moulins and crevasses (Smith et al., 2015; Chudley et al., 2025), which likely would have been the case for the rapidly deglaciating FIS as well. We identified several circular imprints which share similar dimensions and morphologies with the paleo-blisters identified in southwestern Finland (Mäkinen et al., 2023b; Hannula et al., 2024). These depressions in the FLDIL were frequently found on the lee sides of drumlins, distal to topographic highs, within rugged terrain and in the vicinity of murtoo fields. Basal topography perturbations exert control on supraglacial meltwater ponding and crevasse formation depending on the size of the perturbation and thickness of the ice (Gudmundsson, 2003; Ignéczi et al., 2018). This is especially evident under thinner ice closer to the ice sheet margin (Catania et al., 2008), where increased crevassing promotes moulin formation. Topographical control could, at least in part, explain the observed spatial distribution of these features. Due to the similarities in morphology (cf. Mäkinen et al., 2023b), their association with SMCs and their relationship with topography, we suggest that the depressions could be related to inputs of supraglacially derived meltwater. We interpret the circular depressions with radiating outflow channels as potential paleo-blisters formed by highly pressurized water flow (Lai et al., 2021; Mäkinen et al., 2023b), while the depressions associated with a singular, larger down-ice channel could potentially record former moulin locations. One of the circular depressions with a large down-ice channel (Fig. 9B) evidently cross-cuts a hummocky SMC, which likely formed closer to the ice sheet margin (Ahokangas et al., 2021). On the other hand, the co-existence of murtoos and the depressions interpreted as water blisters indicates the depressions formed ~40 to 60 km from the lobe margin (cf. Hepburn et al., 2024), which is consistent with recorded blister formation occurring further inland in western Greenland (Dow et al., 2015; Lai et al., 2021). However, despite similarities to previously described landforms, subglacial origin cannot be confirmed based on geomorphological evidence alone and further analysis requires field-based evidence in combination with closer morphometric analysis. Furthermore, our focus in this study was strictly on SMCs, and a systematic screening of the entire region is needed to determine their distribution both within and outside of meltwater corridors.

Subglacial lakes are widespread under contemporary ice sheets and glaciers (Livingstone et al., 2022). Several studies have described relict subglacial lakes beneath paleo-ice sheets (Livingstone et al., 2012, 2013, 2016) and hydropotential models have demonstrated the potential for meltwater ponding beneath the FIS (Gudlaugsson et al., 2017; Shackleton et al., 2018). Interestingly, Shackleton et al. (2018) predicted several clusters of relatively persistent subglacial lakes located proximal to the topographically higher regions along the western FLDIL margin, particularly proximal to the Toivakka–Konnevesi region. Our results demonstrate that these model predictions closely match the occurrence of the major SMCs indicative of significant sediment erosion in the W sub-lobe and, although in lesser dimensions, in the western SE trunk.

Sedimentological evidence from murtoos has attributed their formation to episodic, seasonal drainage events (Mäkinen et al., 2023a; Hovikoski et al., 2023), and observations from western Greenland show that seasonally active subglacial lakes typically fill via supraglacial inputs and drain during the summer melt season (Bowling et al., 2019; Fan et al., 2023). Numerous murtoo fields and the two notable meltwater complexes within the W sub-lobe are located immediately down-ice of this hypothesized major subglacial lake location. Furthermore, crenulated margins in SMCs and tunnel valleys have been associated with turbulent flow and flooding events (e.g. Rampton, 2000; Livingstone and Clark, 2016; Sharpe et al., 2021), and these features are notably found distal to the Konnevesi bedrock high and the lake Puula basin, from which multiple SMCs with incised morphologies abruptly start. Shackleton et al. (2018) also predicted several small lakes with low persistence potential on the eastern side of the NW trunk, where we found instances of SMCs with murtoos which start abruptly from peat covered areas (Fig. 8E). Livingstone et al. (2016) described shallow subglacial lakes identifiable as flat spots on a paleo-ice sheet bed, which drained via channels incised to the bed substrate. It is possible that SMCs such as the one described here could have formed through drainage of shallow subglacial ponds.

Generally, subglacial water tends to pond in bedrock depressions under shallower ice surface slopes, while steeper slopes and the resulting stronger hydropotential gradient promotes drainage (Pattyn, 2008). In the context of the FLDIL, the orientation of the bedrock regions transverse to the prevalent ice flow direction and hydropotential gradient could have promoted stable water ponding under changing ice sheet geometry. The relict subglacial lakes described by Livingstone et al. (2016) were similarly constrained by upland ridges oriented transverse to the ice flow. According to Shackleton et al. (2018), the flat surfaces of present-day lakes on DEM prevented the prediction of subglacial lakes in these basins. Considering that present-day lakes cover significant portions of our study area the size and distribution of potential subglacial lakes is likely underestimated in the model output. Based on our results, we suggest that, in addition to the area proximal to the Toivakka–Konnevesi region, the present-day Lake Puula basin, the lake Keitele area and the large lake basins at the center of the E sub-lobe may have also been significant subglacial water reservoirs. Interestingly, these hypothesized locations also correspond to the unexpected alternating spatial pattern of overwinter channels produced by the process-based subglacial hydrology model of Hepburn et al. (2024) in the FLDIL lobe. However, the ice lobe geometry and simple climate forcing used in the model may have resulted in higher melt rates and moulin densities being predicted in these outer two-thirds of the lobe, so we are not able to reliably link the model outputs to actual processes regarding subglacial lakes or evaluate the performance of the model based solely on this spatial connection.

5.5. Implications for the deglaciation dynamics of the FLDIL

A few continuous eskers extend from the FLDIL lobe across the trunk, indicating that some SMCs could be somewhat contemporaneous between the regions. However, the marked regional variations in SMC dimensions, spacing and esker associations suggests that they were primarily controlled by a combination of substrate characteristics, ice sheet dynamics and evolving drainage conditions. This interpretation is consistent with previously described deglaciation patterns (Glückert, 1974; Mäkelä, 1988; Ahokangas and Mäkinen, 2014; Lunkka et al., 2021), which we will discuss here in comparison with our results. Our findings are summarized in Fig. 11, to which we refer throughout the text with numbers to indicate relevant map locations.

The FLDIL lobe consisted of two sub-lobes (Punkari, 1980; Ahokangas and Mäkinen, 2014), but details of their behavior are poorly constrained. Prior to the onset of the Holocene epoch at 11.65 cal. Kyr BP (Stroeven et al., 2016), the FLDIL experienced several ice retreat and readvance phases (Fig. 11; 1) (see Lunkka et al., 2021), which likely

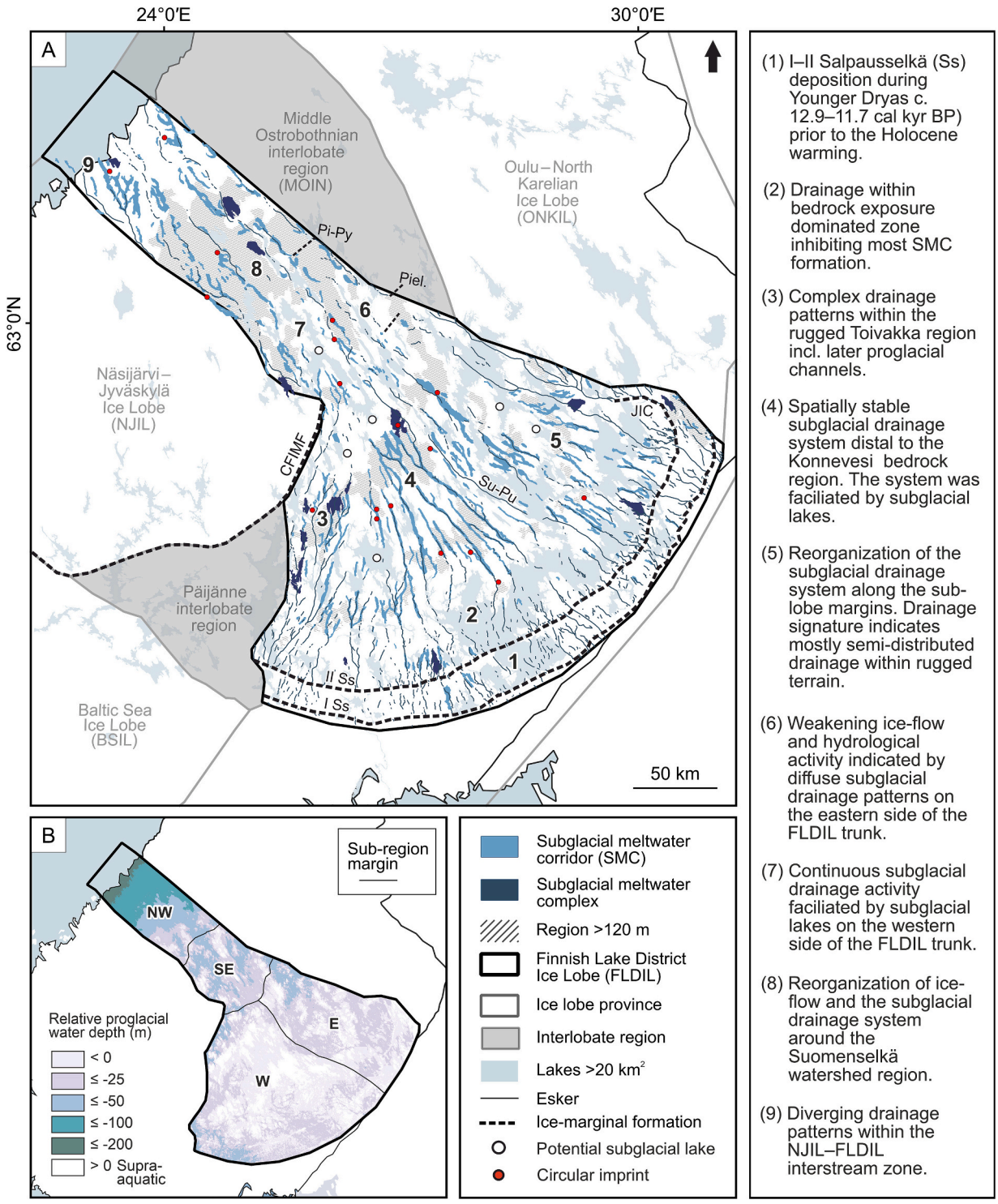

Fig. 11. A) Combined SMC polygon data and esker data illustrating regional drainage patterns and their connection to hypothesized subglacial lake locations and topographically higher regions. The numbered text paragraphs summarize key elements discussed in Section 5.5. Elevation threshold of 120 m was chosen for visualization purposes and is heavily simplified to illustrate the relationship between SMCs, circular imprints and topography. Eskers (polylines) provided by Ahokangas et al. (2021). B) Relative proglacial water depth (Ojala et al., 2013) and sub-region borders. Abbreviations used: I–II Ss = I–II Salpausselkä, CFIMF=Central Finland Ice Marginal Formation, JIC = Jaamankangas interlobate complex, Su–Pu = Suonenjoki–Punkaharju esker, Piel. = Pielavesi end moraine (Glückert, 1974), Pi–Py = Pihtipudas–Pyhäjärvi end moraine (Mäkelä, 1988).

formed the bedrock exposure dominated zone in the W sub-lobe proximal to the II Salpausselkä (Fig. 11; 2).

We observed several aligned meltwater complexes in association with the western interlobate margin in the lobe, where the terrain is rugged, relative elevation differences are high and esker network is dense (Fig. 11; 3). Their occurrence indicates widespread meltwater activity, which was probably related to a combination of topography controlled processes including crevassing and sub- or supraglacial lake drainages. These complexes are oriented away from the ice lobe margin, which could simply result from the steep incline of the terrain toward

the FLDIL interior. However, it is also possible that the neighboring Päijänne interlobate region remained frozen to the bed, which would steer meltwater flow to the interior of the rapidly thinning lobe.

Interestingly, SMCs in the proximity of the Suonenjoki–Punkaharju esker to the east are likewise oriented toward the W-sub-lobe interior instead of the sub-lobe margin, and this cannot be explained by topographic gradient. This contrasts with the adjacent SMCs belonging to the Suonenjoki cluster which turn steeply toward the interlobate joint. This suggests differences in drainage organization and pressure conditions between the sub-lobes. Indeed, a significant change in SMC morphometry and esker association is evident within the E sub-lobe approximately 50–60 km up-ice from the II Salpausselkä where the terrain transitions to rugged topography (Fig. 11; 5). We interpret this change to reflect reorganization of the drainage system toward a distributed to semi-distributed configuration, and this change could be explained by a combination of factors.

The hypothesized subglacial lakes located proximal to the Toivakka–Konnevesi region (cf. Shackleton et al., 2018) would have played an important role in SMC formation and drainage evolution during deglaciation (Fig. 11; 4). Repeated, seasonal inputs from these subglacial lakes, coupled with the bedrock structure within the Pieksämäki region, likely sustained more efficient drainage along the major SMCs in the W sub-lobe. The rugged terrain of the E sub-lobe, on the other hand, would have promoted more spatially variable meltwater delivery and distributed conditions (cf. Lewington et al., 2020) and routed drainage along bedrock depressions toward the sub-lobe margin. The E sub-lobe contains several large lake basins oriented perpendicular to the ice flow in its central part, which we also interpreted as potential subglacial lake locations. However, they may have not been active for the entire duration the region was ice covered.

It is also possible that local variations in proglacial conditions affected ice geometry. The W sub-lobe margin retreated in predominantly terrestrial conditions (Fig. 11B) (Ojala et al., 2013), which could have promoted rapid thinning of the ice margin and sustained steeper hydropotential gradients toward the frontal margin. In contrast, the E sub-lobe likely terminated in locally deeper proglacial water occupying the lake basins proximal to the II Salpausselkä, which could have facilitated faster withdrawal and thinning of the ice.

Changes in subglacial topography resulted in ice flow reorganization over the Suomenselkä watershed region (Ahokangas and Mäkinen, 2014). Prior to this shift in regime, the ice stream trunk was divided into eastern and western flow corridors. The eastern side experienced stagnation and margin oscillation as evidenced by several prominent ice marginal moraines (Glückert, 1974; Mäkelä, 1988). Lewington et al. (2020) hypothesized that less distinct geomorphic expression in SMCs indicates reduced delivery of surface meltwater to the bed. This relationship is evident in the marked decrease in SMC dimensions and density between the lobe and the SE trunk, especially on the eastern side (Fig. 11; 6). Conversely, the mapped drainage patterns and the lack of similar ice-marginal moraine on the western side (Fig. 11; 7) signifies continuous hydrological activity and margin retreat (cf. Glückert, 1974; Mäkelä, 1988). This could have been promoted by subglacial lake activity in the Lake Keitele area (cf. Shackleton et al., 2018) or by enhanced crevassing within the rougher terrain. The comparatively narrow size of the SMCs could indicate lesser subglacial lake volume or activity, or alternatively, reflect rapid ice sheet retreat, which would inhibit the time these SMCs remained active compared to those in the lobe.

We observed significant changes in SMC relief, dimensions and esker association over the Suomenselkä (Fig. 11; 8) and interpret this to reflect a shift toward predominantly distributed to semi-distributed drainage consistent with the previous ice-flow reorganization pattern (Ahokangas and Mäkinen, 2014). Lewington et al. (2020) found sparser and more dendritic drainage patterns under paleo-ice streams and concluded that their generally lower ice surface profiles and resulting hydropotential gradients could favor distributed drainage. In the context of the FLDIL ice stream trunk, the rapidly deepening proglacial water (Fig. 11B) could also have promoted margin flotation, gentler hydropotential gradient and rapid withdrawal of the ice, which would drive meltwater flow locally toward the lower pressure ice-flow zone margins (i.e. major esker chains). It is also notable that the diverging drainage pattern observed in the Bothnian Bay area (Fig. 11; 9) coincides with the hypothesized NJIL–FLDIL interstream zone (Ahokangas and Mäkinen, 2014), where drainage seems to have operated independently from the rest of the NW trunk.

Ahokangas et al. (2021) suggested that meltwater supply within the trunk was mainly generated by shear-induced melting and enhanced crevassing along the ice-flow zone margins. In the context of Antarctic ice streams, where surface-driven melting is often negligible, meltwater flux from temperate shear margins (e.g. Meyer et al., 2018) and basal friction is significant (Ranganathan et al., 2023). In the rapidly deglaciating FLDIL, however, shear-induced melting is unlikely to be the only contributor to SMC formation and we propose that shallow subglacial ponds in the region (cf. Livingstone et al., 2016) could have been another contributing factor.

6. Conclusions

High-resolution LiDAR-based DEMs were used to map and classify subglacial meltwater corridors (SMCs) in the Finnish Lake District Ice Lobe (FLDIL) of the former Fennoscandian Ice Sheet. This paper presents a detailed analysis of their morphometry, relief type, and esker associations. The main conclusions are as follows:

1) The median length of individual SMCs in the FLDIL is 7.5 km, and SMC networks have a median length of 9.7 km. They have a consistent average width of 1 km according to both mean and median values. A median spacing between adjacent SMCs is 5.5 km. The observed positive relationship between SMC length and width might suggest a primarily time-transgressive origin. The overall narrower spacing of SMCs compared to eskers is interpreted to express a predominantly semi-distributed drainage signature.
2) The organization, development and stability of the subglacial drainage system were strongly influenced by regional variations in bedrock topography and glacial overburden thickness. Rugged terrain promoted the formation of dense and complex SMC networks and bedrock depressions lay foundations for spatially stable, long-term drainage pathways. Larger topographic highs and basins facilitated meltwater ponding and contributed to ice flow reorganization during deglaciation. Negative-relief SMC morphologies appear dominant and occur in regions of relatively thicker till cover, indicating considerable sediment removal in the lobate part of the FLDIL. Positive-relief SMCs are commonly associated with the reworking of pre-existing landforms. Spatial variations in SMC–esker associations reflect the same controlling factors and indicate regional differences in dominant drainage configurations.
3) Geomorphological evidence for supraglacial meltwater inputs was identified and occurs primarily in association with topographic highs and on the lee sides of drumlins. Importantly, the spatial distribution of major SMC networks corresponds closely with predicted locations of paleo-subglacial lakes (cf. Shackleton et al., 2018). Subglacial lakes therefore likely formed an active and important component of the hydrological system. This interpretation is further supported by the distribution of murtoo fields, crenulated SMC margins, and the prevalence of erosional corridors down-ice of the locations.
4) Comparisons between regional ice sheet dynamics, corridor morphometry and SMC–esker associations demonstrate how the subglacial drainage system evolved during deglaciation. Large-scale drainage organization was likely driven by changes in bed topography, proglacial conditions and meltwater input. Additionally, our results highlight marked differences between the western and eastern parts of the FLDIL lobe and provide new, significant insights

into the nature of SMCs beneath the Finnish sector of the Fennoscandian Ice Sheet.

CRediT authorship contribution statement

Juulia J. Kautto: Writing – original draft, Visualization, Methodology, Investigation, Funding acquisition, Formal analysis, Conceptualization. **Joni K. Mäkinen:** Writing – review & editing, Supervision, Resources, Methodology, Conceptualization. **Antti E.K. Ojala:** Writing – review & editing, Supervision, Resources, Methodology, Conceptualization.

Declaration of Generative AI and AI-assisted technologies in the writing process

During the preparation of this work the authors used OpenAI's ChatGPT v5.2 solely in order to improve the grammar and readability of specific paragraphs. After using this tool, the authors reviewed and edited the content as needed and take full responsibility for the content of the publication.

Declaration of competing interest

The authors declare that they have no known competing financial interests or personal relationships that could have appeared to influence the work reported in this paper.

Acknowledgements

This work was financially supported by the Doctoral Programme in Biology, Geography and Geology (BGG) of the University of Turku Graduate School (UTUGS) (Juulia J. Kautto) and was conducted with the collaboration of Digital Waters Flagship (DIWA) (decision no. 359247, Research Council of Finland) (Antti E.K. Ojala). We thank one anonymous reviewer and Edouard Ravier for their constructive feedback which helped to improve the quality of the manuscript. The authors would also like to thank Adam Hepburn for his comments that improved the text.

Appendix A. Supplementary data

Supplementary data to this article can be found online at https://doi.org/10.1016/j.geomorph.2026.110319.

Data availability

Data will be made available on request.

References

Ahokangas, E., Mäkinen, J., 2014. Sedimentology of an ice lobe margin esker with implications for the deglacial dynamics of the Finnish Lake District lobe trunk. Boreas 43, 90–116. https://doi.org/10.1111/bor.12023.

Ahokangas, E., Ojala, A.E.K., Tuunainen, A., Valkama, M., Palmu, J.P., Kajuutti, K., Mäkinen, J., 2021. The distribution of glacial meltwater routes and associated murtoo fields in Finland. Geomorphology 389, 107854. https://doi.org/10.1016/j.geomorph.2021.107854.

Andrews, L.C., Catania, G.A., Hoffman, M.J., Gulley, J.D., Lüthi, M.P., Ryser, C., Hawley, R.L., Neumann, T.A., 2014. Direct observations of evolving subglacial drainage beneath the Greenland Ice Sheet. Nature 514, 80–83. https://doi.org/10.1038/nature13796.

Bartholomew, I., Nienow, P., Mair, D., Hubbard, A., King, M.A., Sole, A., 2010. Seasonal evolution of subglacial drainage and acceleration in a Greenland outlet glacier. Nat. Geosci. 3, 408–411. https://doi.org/10.1038/ngeo863.

Boulton, G.S., Hagdorn, M., Maillot, P.B., Zatsepin, S., 2009. Drainage beneath ice sheets: groundwater-channel coupling, and the origin of esker systems from former ice sheets. Quat. Sci. Rev. 28, 621–638. https://doi.org/10.1016/j.quascirev.2008.05.009.

Bowling, J.S., Livingstone, S.J., Sole, A.J., Chu, W., 2019. Distribution and dynamics of Greenland subglacial lakes. Nat. Commun. 10, 2810. https://doi.org/10.1038/s41467-019-10821-w.

Burke, M.J., Brennand, T.A., Perkins, A.J., 2012. Evolution of the subglacial hydrologic system beneath the rapidly decaying Cordilleran Ice Sheet caused by ice-dammed lake drainage: Implications for meltwater-induced ice acceleration. Quat. Sci. Rev. 50, 125–140. https://doi.org/10.1016/j.quascirev.2012.07.005.

Catania, G.A., Neumann, T.A., Price, S.F., 2008. Characterizing englacial drainage in the ablation zone of the Greenland ice sheet. J. Glaciol. 54, 567–578. https://doi.org/10.3189/002214308786570854.

Chudley, T.R., Howat, I.M., King, M.D., MacKie, E.J., 2025. Increased crevassing across accelerating Greenland Ice Sheet margins. Nat. Geosci. 18, 148–153. https://doi.org/10.1038/s41561-024-01636-6.

Clark, C.D., 1993. Mega-scale glacial lineations and cross-cutting ice-flow landforms. Earth Surf. Process. Landf. 18, 1–29. https://doi.org/10.1002/esp.3290180102.

Das, S.B., Joughin, I., Behn, M.D., Howat, I.M., King, M.A., Lizarralde, D., Bhatia, M.P., 2008. Fracture propagation to the base of the Greenland ice sheet during supraglacial lake drainage. Science 320 (5877), 778–781. https://doi.org/10.1126/science.1153360.

Davison, B.J., Sole, A.J., Livingstone, S.J., Cowton, T.R., Nienow, P.W., 2019. The influence of hydrology on the dynamics of land-terminating sectors of the Greenland ice sheet. Front. Earth Sci. 7, 10. https://doi.org/10.3389/feart.2019.00010.

Dewald, N., Livingstone, S.J., Clark, C.D., 2022. Subglacial meltwater routes of the Fennoscandian Ice Sheet. J. Maps 18, 382–396. https://doi.org/10.1080/17445647.2022.2071648.

Dow, C.F., Kulessa, B., Rutt, I.C., Doyle, S.H., Hubbard, A., 2014. Upper bounds on subglacial channel development for interior regions of the Greenland ice sheet. J. Glaciol. 60, 1044–1052. https://doi.org/10.3189/2014JoG14J093.

Dow, C.F., Kulessa, B., Rutt, I.C., Tsai, V.C., Pimentel, S., Doyle, S.H., Van As, D., Lindbäck, K., Pettersson, R., Jones, G.A., Hubbard, A., 2015. Modeling of subglacial hydrological development following rapid supraglacial lake drainage. J. Geophys. Res. Earth Surf. 120, 1127–1147. https://doi.org/10.1002/2014JF003333.

Dulfer, H.E., Boyes, B.M., Clark, C.D., Dewald, N., Butcher, F.E.G., Ely, J.C., Hughess, A.L.C., 2026. Geomorphological characterisation, pattern, and distribution of ice-margin positions of the former Scandinavian Ice Sheet. Geomorphology 499, 110194. https://doi.org/10.1016/j.geomorph.2026.110194.

Dunlop, P., Clark, C.D., 2006. The morphological characteristics of ribbed moraine. Quat. Sci. Rev. 25, 1668–1691. https://doi.org/10.1016/J.QUASCIREV.2006.01.002.

Fan, Y., Ke, C.Q., Shen, X., Xiao, Y., Livingstone, S.J., Sole, A.J., 2023. Subglacial lake activity beneath the ablation zone of the Greenland Ice Sheet. Cryosphere 17, 1775–1786. https://doi.org/10.5194/tc-17-1775-2023.

Fountain, A.G., Walder, J.S., 1998. Water flow through temperate glaciers. Rev. Geophys. 36, 299–328. https://doi.org/10.1029/97RG03579.

Frydrych, M., Ahokangas, E., Mäkinen, J., Lejzerowicz, A., 2025. Morphological characteristics of eskers in areas with soft and hard bed: Examples from Poland and Finland. Quat. Int. 717, 109649. https://doi.org/10.1016/J.QUAINT.2024.109649.

[Dataset] Geological Survey of Finland, 2010. Superficial deposits of Finland 1:200 000 (sediment polygons). https://tupa.gtk.fi/paikkatieto/meta/maapera_200k.html.

[Dataset] Geological Survey of Finland, 2013. Ancient shorelines. https://tupa.gtk.fi/paikkatieto/meta/ancient_shorelines.html.

[Dataset] Geological Survey of Finland, 2016. Superficial deposits of Finland 1:1 000 000. https://tupa.gtk.fi/paikkatieto/meta/maapera_1m.html.

[Dataset] Geological Survey of Finland, 2021. Glacial features. https://tupa.gtk.fi/paikkatieto/meta/glacial_features.html.

Glückert, G., 1973. Two large drumlin fields in Central Finland. Fennia 120, 1–37. https://fennia.journal.fi/article/view/9238.

Glückert, G., 1974. On deglaciation between Pieksämäki and Pielavesi in Central Finland. Bull. Geol. Soc. Finl. 46, 43–51. https://doi.org/10.17741/bgsf/46.1.007.

Greenwood, S.L., Clark, C.D., Hughes, A.L.C., 2007. Formalising an inversion methodology for reconstructing ice-sheet retreat patterns from meltwater channels: Application to the British Ice Sheet. J. Quat. Sci. 22, 637–645. https://doi.org/10.1002/jqs.1083.

Greenwood, S.L., Clason, C.C., Helanow, C., Margold, M., 2016. Theoretical, contemporary observational and palaeo-perspectives on ice sheet hydrology: Processes and products. Earth Sci. Rev. 155, 1–27. https://doi.org/10.1016/j.earscirev.2016.01.010.

Gudlaugsson, E., Humbert, A., Andreassen, K., Clason, C.C., Kleiner, T., Beyer, S., 2017. Eurasian ice-sheet dynamics and sensitivity to subglacial hydrology. J. Glaciol. 63, 556–564. https://doi.org/10.1017/jog.2017.21.

Gudmundsson, G.H., 2003. Transmission of basal variability to a glacier surface. J. Geophys. Res. Solid Earth 108, 2253. https://doi.org/10.1029/2002jb002107.

Hannula, M., Korkiakoski, K., Ryttäri, S., Virtanen, V., Mäkinen, J., Ojala, A.E.K., 2024. Jäätikön sulamisvesien jäljet Satakunnan kumpumoreenialueella: potentiaalisten paleoblisterien kartoitus. GEOLOGI 76, 88–101.

Hepburn, A.J., Dow, C.F., Ojala, A., Mäkinen, J., Ahokangas, E., Hovikoski, J., Palmu, J.-P., Kajuutti, K., 2024. The organization of subglacial drainage during the demise of the Finnish Lake District Ice Lobe. Cryosphere 18, 4873–4916. https://doi.org/10.5194/tc-18-4873-2024.

Hewitt, I.J., 2011. Modelling distributed and channelized subglacial drainage: the spacing of channels. J. Glaciol. 57, 302–314. https://doi.org/10.3189/002214311796405951.

Hoffman, M.J., Andrews, L.C., Price, S.A., Catania, G.A., Neumann, T.A., Lüthi, M.P., Gulley, J., Ryser, C., Hawley, R.L., Morriss, B., 2016. Greenland subglacial drainage evolution regulated by weakly connected regions of the bed. Nat. Commun. 7, 13903. https://doi.org/10.1038/ncomms13903.

Hooke, R.LeB., 2019. Principles of Glacier Mechanics, 3rd ed. Cambridge University Press. https://doi.org/10.1017/9781108698207.

Hovikoski, J., Mäkinen, J., Winsemann, J., Soini, S., Kajuutti, K., Hepburn, A., Ojala, A.E.K., 2023. Upper-flow regime bedforms in a subglacial triangular-shaped landform

(murtoo), Late Pleistocene, SW Finland: Implications for flow dynamics and sediment transport in (semi-) distributed subglacial meltwater drainage systems. Sediment. Geol. 454, 106448. https://doi.org/10.1016/j.sedgeo.2023.106448.
Hubbard, B., Nienow, P., 1997. Alpine subglacial hydrology. Quat. Sci. Rev. 16, 939–955. https://doi.org/10.1016/S0277-3791(97)00031-0.
Ignéczi, Á., Sole, A.J., Livingstone, S.J., Ng, F.S.L., Yang, K., 2018. Greenland Ice Sheet Surface Topography and Drainage Structure Controlled by the Transfer of Basal Variability. Front. Earth Sci. 6, 101. https://doi.org/10.3389/feart.2018.00101.
Jennes, J., 2013. DEM surface tools. Jennes Enterprises Available at. https://www.jennessent.com/arcgis/surface_area.htm.
Kajuutti, K., Mäkinen, J., Palmu, J.-P., 2016. LiDAR-based interpretation of deglacial dynamics in SW Finland. In: Staubolis, S., Karvonen, T., Kujanpää, A. (Eds.), Abstracts of the 32nd Nordic Geological Winter Meeting 13-15th January 2016, Bull. Geol. Soc. Finl., Helsinki, Finland, p. 314.
Krabbendam, M., Bradwell, T., 2014. Quaternary evolution of glaciated gneiss terrains: pre-glacial weathering vs. glacial erosion. Quat. Sci. Rev. 95, 20–42. https://doi.org/10.1016/j.quascirev.2014.03.013.
Krabbendam, M., Eyles, N., Putkinen, N., Bradwell, T., Arbelaez-Moreno, L., 2016. Streamlined hard beds formed by palaeo-ice streams: A review. Sediment. Geol. 338, 24–50. https://doi.org/10.1016/J.SEDGEO.2015.12.007.
Lai, C.Y., Stevens, L.A., Chase, D.L., Creyts, T.T., Behn, M.D., Das, S.B., Stone, H.A., 2021. Hydraulic transmissivity inferred from ice-sheet relaxation following Greenland supraglacial lake drainages. Nat. Commun. 12, 3955. https://doi.org/10.1038/s41467-021-24186-6.
Lewington, E.L.M., Livingstone, S.J., Sole, A.J., Clark, C.D., Ng, F.S.L., 2019. An automated method for mapping geomorphological expressions of former subglacial meltwater pathways (hummock corridors) from high resolution digital elevation data. Geomorphology 339, 70–86. https://doi.org/10.1016/j.geomorph.2019.04.013.
Lewington, E.L.M., Livingstone, S.J., Clark, C.D., Sole, A.J., Storrar, R.D., 2020. A model for interaction between conduits and surrounding hydraulically connected distributed drainage based on geomorphological evidence from Keewatin, Canada. Cryosphere 14, 2949–2976. https://doi.org/10.5194/tc-14-2949-2020.
Livingstone, S.J., Clark, C.D., 2016. Morphological properties of tunnel valleys of the southern sector of the Laurentide Ice Sheet and implications for their formation. Earth Surf. Dyn. 4, 567–589. https://doi.org/10.5194/esurf-4-567-2016.
Livingstone, S.J., Clark, C.D., Piotrowski, J.A., Tranter, M., Bentley, M.J., Hodson, A., Swift, D.A., Woodward, J., 2012. Theoretical framework and diagnostic criteria for the identification of palaeo-subglacial lakes. Quat. Sci. Rev. 53, 88–110. https://doi.org/10.1016/j.quascirev.2012.08.010.
Livingstone, S.J., Clark, C.D., Tarasov, L., 2013. Modelling North American palaeo-subglacial lakes and their meltwater drainage pathways. Earth Planet. Sci. Lett. 375, 13–33. https://doi.org/10.1016/j.epsl.2013.04.017.
Livingstone, S.J., Utting, D.J., Ruffell, A., Clark, C.D., Pawley, S., Atkinson, N., Fowler, A. C., 2016. Discovery of relict subglacial lakes and their geometry and mechanism of drainage. Nat. Commun. 7, ncomms11767. https://doi.org/10.1038/ncomms11767.
Livingstone, S.J., Li, Y., Rutishauser, A., Sanderson, R.J., Winter, K., Mikucki, J.A., Björnsson, H., Bowling, J.S., Chu, W., Dow, C.F., Fricker, H.A., McMillan, M., Ng, F. S.L., Ross, N., Siegert, M.J., Siegfried, M., Sole, A.J., 2022. Subglacial lakes and their changing role in a warming climate. Nat. Rev. Earth Environ. 3, 106–124. https://doi.org/10.1038/s43017-021-00246-9.
Lunkka, J.P., Erkkilä, A., 2012. Behaviour of the lake district ice lobe of the Scandinavian ice sheet during the younger dryas chronozone (ca. 12 800-11 500 years ago). In: POSIVA Working Report 2012-17, p. 54.
Lunkka, J.P., Palmu, J.P., Seppänen, A., 2021. Deglaciation dynamics of the Scandinavian Ice Sheet in the Salpausselkä zone, southern Finland. Boreas 50, 404–418. https://doi.org/10.1111/bor.12502.
Mäkelä, J., 1988. Deglasiaatio Kinnulan-Pihtiputaan alueella Keski-Suomessa. [Deglaciation in the Kinnula-Pihtipudas area in Central Finland]. In: Publications of the Department of Quaternary Geology, 62. University of Turku, p. 39, 2 app.
Mäkinen, J., 2003. Time-transgressive deposits of repeated depositional sequences within interlobate glaciofluvial (esker) sediments in Köyliö, SW Finland. Sedimentology 50, 327–360. https://doi.org/10.1046/j.1365-3091.2003.00557.x.
Mäkinen, J., Kajuutti, K., Palmu, J.P., Ojala, A., Ahokangas, E., 2017. Triangular-shaped landforms reveal subglacial drainage routes in SW Finland. Quat. Sci. Rev. 164, 37–53. https://doi.org/10.1016/j.quascirev.2017.03.024.
Mäkinen, J., Kajuutti, K., Ojala, A.E.K., Ahokangas, E., Tuunainen, A., Valkama, M., Palmu, J.P., 2023a. Genesis of subglacial triangular-shaped landforms (murtoos) formed by the Fennoscandian Ice Sheet. Earth Surf. Process. Landf. 48, 2171–2196. https://doi.org/10.1002/esp.5606.
Mäkinen, J., Dow, C.F., Ahokangas, E., Ojala, A., Kajuutti, K., Kautto, J., Palmu, J.P., 2023b. Water blister geomorphology and subglacial drainage sediments: an example from the bed of the Fennoscandian Ice Sheet in SW Finland. J. Glaciol. 69, 1529–1545. https://doi.org/10.1017/jog.2023.37.
Meyer, C.R., Yehya, A., Minchew, B., Rice, J.R., 2018. A model for the downstream evolution of temperate ice and subglacial hydrology along ice stream shear margins. J. Geophys. Res. Earth Surf. 123, 1682–1698. https://doi.org/10.1029/2018JF004669.
Möller, P., 2006. Rogen moraine: an example of glacial reshaping of pre-existing landforms. Quat. Sci. Rev. 25, 362–389. https://doi.org/10.1016/j.quascirev.2005.01.011.
Ojala, A.E.K., Palmu, J.P., Åberg, A., Åberg, S., Virkki, H., 2013. Development of an ancient shoreline database to reconstruct the Litorina Sea maximum extension and the highest shoreline of the Baltic Sea basin in Finland. Bull. Geol. Soc. Finl. 85, 127–144. https://doi.org/10.17741/bgsf/85.2.002.
Ojala, A.E.K., Mäkinen, J., Ahokangas, E., Kajuutti, K., Valkama, M., Tuunainen, A., Palmu, J.P., 2021. Diversity of murtoos and murtoo-related subglacial landforms in the Finnish area of the Fennoscandian Ice Sheet. Boreas 50, 1095–1115. https://doi.org/10.1111/bor.12526.
Ojala, A.E.K., Mäkinen, J., Kajuutti, K., Ahokangas, E., Palmu, J.P., 2022. Subglacial evolution from distributed to channelized drainage: Evidence from the Lake Murtoo area in SW Finland. Earth Surf. Process. Landf. 47, 2877–2896. https://doi.org/10.1002/esp.5430.
Palmer, S., Mcmillan, M., Morlighem, M., 2015. Subglacial lake drainage detected beneath the Greenland ice sheet. Nat. Commun. 6, 8408. https://doi.org/10.1038/ncomms9408.
Palmu, J.P., Ojala, A.E.K., Ruskeeniemi, T., Sutinen, R., Mattila, J., 2015. LiDAR DEM detection and classification of postglacial faults and seismically-induced landforms in Finland: a paleoseismic database. GFF 137, 344–352. https://doi.org/10.1080/11035897.2015.1068370.
Palmu, J.P., Ojala, A.E.K., Virtasalo, J., Putkinen, N., Kohonen, J., Sarala, P., 2021. Classification system for superficial (quaternary) geological units in Finland. Bull. Geol. Soc. Finl. 412, 115–169. https://doi.org/10.30440/bt412.4.
Palmu, J.-P., Pitkäranta, R., Hovikoski, J., Ojala, A., Valkama, M., Väänänen, T., 2026. Salpausselkien alueen yhteenvetoraportti. [Summary: overview report of the Salpausselkä Area. Geological Survey of Finland]. In: Open File Research Report 1/2026, p. 153.
Pattyn, F., 2008. Investigating the stability of subglacial lakes with a full Stokes ice-sheet model. J. Glaciol. 54, 353–361. https://doi.org/10.3189/002214308784886171.
Peterson, G., Johnson, M.D., 2018. Hummock corridors in the south-central sector of the Fennoscandian ice sheet, morphometry and pattern. Earth Surf. Process. Landf. 43, 919–929. https://doi.org/10.1002/esp.4294.
Peterson, G., Johnson, M.D., Smith, C.A., 2017. Glacial geomorphology of the south Swedish uplands – focus on the spatial distribution of hummock tracts. J. Maps 13, 534–544. https://doi.org/10.1080/17445647.2017.1336121.
Punkari, M., 1980. The ice lobes of the Scandinavian ice sheet during the deglaciation in Finland. Boreas 9, 307–310. https://doi.org/10.1111/j.1502-3885.1980.tb00710.x.
Putkinen, N., Eyles, N., Putkinen, S., Ojala, A.E.K., Palmu, J.P., Sarala, P., Väänänen, T., Räisänen, J., Saarelainen, J., Ahtonen, N., Rönty, H., Kiiskinen, A., Rauhaniemi, T., Tervo, T., 2017. High-resolution LiDAR mapping of glacial landforms and ice stream lobes in Finland. Bull. Geol. Soc. Finl. 89, 64–81. https://doi.org/10.17741/bgsf/89.2.001.
Rampton, V.N., 2000. Large-scale effects of subglacial meltwater flow in the southern Slave Province, Northwest Territories, Canada. Can. J. Earth Sci. 37, 81–93. https://doi.org/10.1139/e99-110.
Ranganathan, M., Barotta, J.-W., Meyer, C.R., Minchew, B., 2023. Meltwater generation in ice stream shear margins: case study in Antarctic ice streams. Proc. A. 479, 20220473. https://doi.org/10.1098/rspa.2022.0473.
Röthlisberger, H., 1972. Water Pressure in Intra- and Subglacial Channels. J. Glaciol. 11, 177–203. https://doi.org/10.3189/s0022143000022188.
Ruuska, E., Skyttä, P., Putkinen, N., Valjus, T., 2023. Contribution of bedrock structures to the bedrock surface topography and groundwater flow systems within deep glaciofluvial aquifers in Kurikka, Western Finland. Earth Surf. Process. Landf. 48, 2039–2056. https://doi.org/10.1002/esp.5602.
Sarala, P., 2025. Characteristic features and formation processes of ribbed moraines. Quat. Int. 741, 109953. https://doi.org/10.1016/j.quaint.2025.109953.
Schoof, C., 2010. Ice-sheet acceleration driven by melt supply variability. Nature 468, 803–806. https://doi.org/10.1038/nature09618.
Schoof, C., 2023. The evolution of isolated cavities and hydraulic connection at the glacier bed – Part 1: Steady states and friction laws. Cryosphere 17, 4797–4815. https://doi.org/10.5194/tc-17-4797-2023.
Sergienko, O.V., Hindmarsh, R.C.A., 2013. Regular patterns in frictional resistance of ice-stream beds seen by surface data inversion. Science 342, 1086–1089. https://doi.org/10.1126/science.1243903.
Shackleton, C., Patton, H., Hubbard, A., Winsborrow, M., Kingslake, J., Esteves, M., Andreassen, K., Greenwood, S.L., 2018. Subglacial water storage and drainage beneath the Fennoscandian and Barents Sea ice sheets. Quat. Sci. Rev. 201, 13–28. https://doi.org/10.1016/j.quascirev.2018.10.007.
Sharpe, D.R., Lesemann, J.E., Knight, R.D., Kjarsgaard, B.A., 2021. Regional stagnation of the western Keewatin ice sheet and the significance of meltwater corridors and eskers, Northern Canada. Can. J. Earth Sci. 58, 1005–1026. https://doi.org/10.1139/cjes-2020-0136.
Shepherd, A., Hubbard, A., Nienow, P., King, M., McMillan, M., Joughin, I., 2009. Greenland ice sheet motion coupled with daily melting in late summer. Geophys. Res. Lett. 36, L01501. https://doi.org/10.1029/2008GL035758.
Shreve, R.L., 1972. Movement of Water in Glaciers. J. Glaciol. 11, 205–214. https://doi.org/10.3189/s002214300002219x.
Simkins, L.M., Greenwood, S.L., Winsborrow, M.C.M., Bjarnadóttir, L.R., Lepp, A.P., 2022. Advances in understanding subglacial meltwater drainage from past ice sheets. Ann. Glaciol. 63, 83–87. https://doi.org/10.1017/aog.2023.16.
Skyttä, P., Kinnunen, J., Palmu, J.P., Korkka-Niemi, K., 2015. Bedrock structures controlling the spatial occurrence and geometry of 1.8 Ga younger glacifluvial deposits — example from First Salpausselkä, southern Finland. Glob. Planet. Chang. 135, 66–82. https://doi.org/10.1016/J.GLOPLACHA.2015.10.007.
Skyttä, P., Nordbäck, N., Ojala, A.E.K., Putkinen, N., Aaltonen, I., Engström, J., Mattila, J., Ovaskainen, N., 2023. The interplay of bedrock fractures and glacial erosion in defining the present-day land surface topography in mesoscopically isotropic crystalline rocks. Earth Surf. Process. Landf. 48, 1956–1968. https://doi.org/10.1002/esp.5596.
Smith, L.C., Chu, V.W., Yang, K., Gleason, C.J., Pitcher, L.H., Rennermalm, A.K., Legleiter, C.J., Behar, A.E., Overstreet, B.T., Moustafa, S.E., Tedesco, M., Forster, R.

R., LeWinter, A.L., Finnegan, D.C., Sheng, Y., Balog, J., 2015. Efficient meltwater drainage through supraglacial streams and rivers on the southwest Greenland ice sheet. Proc. Natl. Acad. Sci. USA 112, 1001–1006. https://doi.org/10.1073/pnas.1413024112.

Stokes, C.R., Margold, M., Creyts, T.T., 2016. Ribbed bedforms on palaeo-ice stream beds resemble regular patterns of basal shear stress ('traction ribs') inferred from modern ice streams. J. Glaciol. 62, 696–713. https://doi.org/10.1017/jog.2016.63.

St-Onge, D., 1984. Surficial deposits of the Redrock Lake area, district of Mackenzie. Curr. Res. Geological Survey of Canada 84-1A, 271–278. https://doi.org/10.4095/119675.

Storrar, R.D., Stokes, C.R., Evans, D.J.A., 2014. Morphometry and pattern of a large sample (>20,000) of Canadian eskers and implications for subglacial drainage beneath ice sheets. Quat. Sci. Rev. 105, 1–25. https://doi.org/10.1016/J.QUASCIREV.2014.09.013.

Stroeven, A.P., Hättestrand, C., Kleman, J., Heyman, J., Fabel, D., Fredin, O., Goodfellow, B.W., Harbor, J.M., Jansen, J.D., Olsen, L., Caffee, M.W., Fink, D., Lundqvist, J., Rosqvist, G.C., Strömberg, B., Jansson, K.N., 2016. Deglaciation of Fennoscandia. Quat. Sci. Rev. 147, 91–121. https://doi.org/10.1016/j.quascirev.2015.09.016.

Tuunainen, A., 2018. Subglasiaaliset järvet osana Lounais-Suomen glasiaalidynamiikkaa? [Effects of subglacial lakes on glacier dynamics in Southwest Finland?]. Master's Thesis. University of Turku, Faculty of Science and Engineering, Department of Geography and Geology 110 pp., 1 app. http://urn.fi/URN:NBN:fi-fe2018112048685.

Utting, D.J., Ward, B.C., Little, E.C., 2009. Genesis of hummocks in glaciofluvial corridors near the Keewatin Ice Divide, Canada. Boreas 38, 471–481. https://doi.org/10.1111/j.1502-3885.2008.00074.x.

Vérité, J., Ravier, E., Bourgeois, O., Bessin, P., Livingstone, S.J., Clark, C.D., Pochat, S., Mourgues, R., 2022. Formation of murtoos by repeated flooding of ribbed bedforms along subglacial meltwater corridors. Geomorphology 408, 108248. https://doi.org/10.1016/j.geomorph.2022.108248.

Vérité, J., Livingstone, S.J., Ravier, E., McMartin, I., Campbell, J., Lewington, E.L.M., Dewald, N., Clark, C.D., Sole, A.J., Storrar, R.D., 2024a. Conceptual model for the formation of bedforms along subglacial meltwater corridors (SMCs) by variable ice-water-bed interactions. Earth Surf. Process. Landf. 49, 170–196. https://doi.org/10.1002/esp.5725.

Vérité, J., Ravier, E., Bourgeois, O., Pochat, S., Bessin, P., 2024b. The kinematic significance of subglacial bedforms and their use in palaeo-glaciological reconstructions. Earth Planet. Sci. Lett. 626, 118510. https://doi.org/10.1016/j.epsl.2023.118510.

Walker, M., Johnsen, S., Rasmussen, S.O., Popp, T., Steffensen, J.P., Gibbard, P., Hoek, W., Lowe, J., Andrews, J., Björck, S., Cwynar, L.C., Hughen, K., Kershaw, P., Kromer, B., Litt, T., Lowe, D.J., Nakagawa, T., Newnham, R., Schwander, J., 2009. Formal definition and dating of the GSSP (Global Stratotype Section and Point) for the base of the Holocene using the Greenland NGRIP ice core, and selected auxiliary records. J. Quat. Sci. 24, 3–17. https://doi.org/10.1002/jqs.1227.

Willis, M.J., Herried, B.G., Bevis, M.G., Bell, R.E., 2015. Recharge of a subglacial lake by surface meltwater in northeast Greenland. Nature 518, 223–227. https://doi.org/10.1038/nature14116.